

212 F

Final Report

10/18/66 to 8/18/70

STUDY OF THE SYNTHESIS OF BLOCK COPOLYMERS

Prepared for:

JET PROPULSION LABORATORY
4800 OAK GROVE DRIVE
PASADENA, CALIFORNIA 91103

CONTRACT NAS 7-523

FACILITY FORM 602

N71-20152
(ACCESSION NUMBER)
94
(PAGES)
CR-117305
(NASA CR OR TMX OR AD NUMBER)

(THRU)

G3

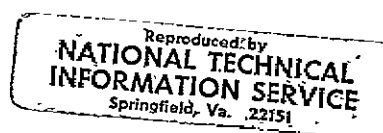
(CODE)

06

(CATEGORY)



STANFORD RESEARCH INSTITUTE
Menlo Park, California 94025 • U.S.A.





STANFORD RESEARCH INSTITUTE
Menlo Park, California 94025 • U.S.A.

Final Report

September 1970

10/18/66 to 8/18/70

STUDY OF THE SYNTHESIS OF BLOCK COPOLYMERS

By J HELLER

Prepared for

JET PROPULSION LABORATORY
4800 OAK GROVE DRIVE
PASADENA, CALIFORNIA 91103

CONTRACT NAS 7-523

SRI Project PRU 6297

Approved by

MARION E HILL, *Director*
Physical Sciences (Chemistry)

CHARLES J COOK *Executive Director*
Physical Sciences Division

PREFACE AND SUMMARY OF ACCOMPLISHMENTS

The basic objective of this research program was to evolve a technology that could lead to an eventual fabrication of bladder materials that are impervious to hydrazine and to nitrogen tetroxide and which are capable of containing these with none, or very little permeation.

The approach which has been pursued was that of block copolymer synthesis and their physical characterization as to structure and permeation parameters.

The following objectives have been achieved.

1. The feasibility of preparing fully fluorinated ABA block copolymers has been demonstrated and a patent application is now being prepared. However, the technology of producing a useful material has not been developed.

2. A synthetic technique has been evolved which is capable of producing ABA block copolymers having a structural purity of at least 95%.

3. A Gel Permeation Chromatography procedure has been worked out whereby the composition of ABA block copolymers can be quantitatively determined.

4. A new permeation instrument has been developed under joint funding from NASA, Stanford Research Institute and the Dohrman Instrument Company. The instrument, which is now commercially available, represents a significant advance which will be of material benefit to the polymer industry as a whole.

5. Two manuscripts have been published.

- (a) Synthesis of 4-Vinylbiphenyl-Isoprene Block Copolymers and their Characterization by Gel-Permeation Chromatography, in J. Polymer Sci. A-1, 7, 73 (1969).

- (b) A Dynamic Approach to Diffusion and Permeation Measurements, in J. Polymer Sci. A-2, 8, 467 (1970).

CONTENTS

GENERAL INTRODUCTION	1
PHASE I	3
I INTRODUCTION	3
II SUMMARY	5
III DISCUSSION	7
1 Preliminary considerations	7
2 Coupling Studies	8
3. Block Copolymer Synthesis	11
4 Polymer Characterization	14
5. Mechanical Properties	21
6 Permeation and Diffusion Studies	22
IV EXPERIMENTAL	29
1. Apparatus	29
2. Purification of Materials	29
a. Isoprene	29
b 4-Vinylbiphenyl	30
c. Sodium Naphthalene	31
d Butyllithium	31
e Phosgene	32
3 Block Copolymer Synthesis	32
4 Polymer Characterization	33
5 Mechanical Property Measurements	33
a Film Casting	33
b Stress-Strain Data	34
6. Diffusion Studies	34
a Film Casting	34
b Permeation Studies	34
REFERENCES	35

CONTENTS

PHASE II

I	INTRODUCTION	37
II	SUMMARY	37
III	DISCUSSION	39
A	α, β, β -Trifluorostyrene	39
1	Anionic Polymerization	39
2	Free Radical Polymerization	42
B	Nitroso Rubber	43
1	General Considerations	43
2	Characterization of Nitroso Rubber	45
3	Cleavage Experiments	46
a	Ultraviolet	46
b	γ -Rays	47
4	Copolymerization Experiments	48
5	Characterization of Copolymer	48
a	Fractionation	48
b	Mutual Solvent	51
c	Composition	52
d	Molecular Weight	52
e	Mechanical Properties	54
IV	EXPERIMENTAL	55
A.	α, β, β -Trifluorostyrene	55
1	Anionic Polymerization	55
2	Free Radical Polymerization	55
3	End-Group Reactions of Amino-Terminated PTFS	55
B	Nitroso Rubber	57
1.	Fractionation	57
2	Irradiation	57
a	Ultraviolet	57
b	X-Ray	58
3	Copolymerization Experiments	58
	REFERENCES	59
	APPENDIX	A-1

TABLES

PHASE I

I	Coupling of Polyisoprene Anions with Reactive Dihalides	9
II	Synthesis of AB and BA Block Copolymers	12
III	Preparation of 4-vinylbiphenyl Isoprene Block Copolymers	13
IV	Characterization of 4-vinylbiphenyl Isoprene ABBA Block Copolymers	18
V	Stress-Strain Properties of Poly-4-vinylbiphenyl Poly Polyisoprene ABA Block Copolymers	22
VI	Characterization of Shell Block Copolymers	24
VII	Preparation and Permeation Data for Thin Films of SBS Block Copolymers Cast from 90/10 Benzene/Heptane	25
VIII	Preparation and Permeation Data for Thin Films of SBS Block Copolymers Cast from Carbon Tetrachloride	26

PHASE II

I	Attempts to Anionically Polymerize α,β,β -Trifluorostyrene at -50°C	40
II	Attempts to Anionically Polymerize α,β,β -Trifluorostyrene at Various Temperatures	41
III	Emulsion Polymerization of Trifluorostyrene	44
IV	Results of Irradiation of Nitroso Rubber in Freon TF	47
V	Gamma Irradiation of Fractionated Nitroso Rubber	49
VI	Block Copolymerization Experiments	50
VII	Screening of Potential Common Solvents for FNR and KEL-F	53

ILLUSTRATIONS

PHASE I

1	GPC of Coupled Polyisoprene Segments	10
2	Construction of Phosgene Tube	11
3	Ultraviolet Absorption at 2575 Å of Poly-4-vinylbiphenyl in Tetrahydrofuran as a Function of Concentration	15
4	Refractive Index Increments in Toluene of 4-vinylbiphenyl-Isoprene Block Copolymers as a Function of Weight Percent of 4-vinylbiphenyl	16
5	GPC of Poly-4-vinylbiphenyl A Segment	19
6	GPC of Poly-4-vinylbiphenyl-polyisoprene AB Segment	20
7	GPC of Poly-4-vinylbiphenyl-polyisoprene ABBA Block Copolymer	21
8	Schematic Diagram of Vacuum System	29
9	Apparatus for Purification of 4-vinylbiphenyl	30
10	Reactor for Preparation of Sodium Naphthalene	31
11	Polymerization Apparatus	32

PRECEDING PAGE BLANK NOT FILMED

GENERAL INTRODUCTION

One of the problems with present elastomers is that although the backbone may be stable, the chemically introduced crosslink is not. However, it has recently been shown that crosslinks can be introduced without a chemical reaction by creating a tri-block material such as styrene-butadiene-styrene copolymers in which the two end segments are incompatible with the center segment and which, in addition, have a high glass temperature, T_g . When the polymer is heated above the T_g of the end blocks, the material becomes fluid and can be molded. But as it cools, the end blocks precipitate out as liquid droplets that become glass-like below T_g . The rubbery center segment is "tied-down" at each end, and so the droplets of glassy material act as the crosslinks. Very strong elastomers can thus be made, without recourse to chemical vulcanization. This elimination of a reactive site also eliminates a potential site of degradation.

A rubbery material can never be completely impermeable. Nevertheless, this type of block copolymer does offer a new means of modifying permeation rates, for, if the end groups are appropriately sized, individual droplets do not form on cooling from the melt, instead, a kind of three-dimensional structure results. Diffusion through this glassy structure will be far slower than through the rubber, and therefore control over the precipitated domains and the morphology of the resulting material offers a new means of permeation control. It is this combination of properties that makes block copolymers a promising area for further technological development.

Work performed during this research program can be divided into two phases which at times were carried out concurrently. The first was concerned with the synthesis of 4-vinylbiphenyl-isoprene ABA block copolymers, a detailed characterization of these materials, and attempts to influence

permeation rates by changes in morphology. The second phase was concerned with the synthesis of ABA block copolymers containing no C-H bonds.

PHASE I

I INTRODUCTION

Although it is recognized that an all-hydrocarbon system could not be used in applications involving nitrogen tetroxide, it was decided that the study of ABA block copolymers, where A represents a poly-4-vinylbiphenyl segment and B represents a polyisoprene segment, would provide a useful way to investigate the feasibility of controlling morphology and its effect on permeation. The above vinylaromatic segment was selected primarily because of experience gained in the polymerization of such systems acquired during previous work for the Jet Propulsion Laboratory under Contract 951326 under NAS 7-100.

In addition to providing a model for permeation studies, the block copolymers synthesized under this contract were also considered as novel propellant binders. Thus, ABA block copolymers can be considered as filled elastomers where A, the vinylaromatic segment, acts as a filler. Since solid propellants are materials that are highly loaded with inorganic materials, it is of interest to minimize the amount of vinylaromatic filler in the block so that a maximum amount of inorganic filler can be incorporated. Use of a high glass transition material such as poly-2-vinylnaphthalene or poly-4-vinylbiphenyl might enable us to use low molecular weight vinylaromatic segments and still have a glass transition temperature close to that of polystyrene. This would enable the preparation of ABA materials that have very short A segments and that still retain useful mechanical properties.

II SUMMARY

A synthetic procedure was developed for the preparation of pure ABA block copolymers of 4-vinylbiphenyl and isoprene. Early attempts involved the initiation of isoprene with sodium naphthalene in tetrahydrofuran and use of the difunctional polyisoprene to initiate polymerization of 4-vinylbiphenyl. However, difficulties in achieving a rigorous purification of 4-vinylbiphenyl and the undesirable 1,2-3,4-microstructure of the polyisoprene led us to abandon this approach in favor of a butyllithium-initiated polymerization in benzene.

Our inability to rigorously purify 4-vinylbiphenyl led to the decision to initiate the polymerization of the vinylaromatic monomer with n-butyllithium in benzene, allow the polymerization to go to completion, add isoprene, and then couple the AB anion with phosgene to an ABBA block copolymer. In this approach the residual impurities in the vinylaromatic monomer do not lead to homopolymer contamination but merely destroy some of the n-butyllithium initiator. By estimating the degree of purity, it is not difficult to use a slight excess of initiator and thus compensate for the amount destroyed. The coupling procedure has been worked out so that couplings in excess of 95 percent could routinely be achieved.

A detailed procedure for a quantitative analysis of the block copolymer using gel permeation chromatography (GPC) has been worked out. The procedure takes into account the different refractive indices of the two homopolymers. This is necessary because GPC uses a differential refractometer as a detector.

Preliminary data have been obtained on the mechanical properties of a series of block copolymers having varying weight percentages of 4-vinylbiphenyl. The results indicate that, unlike styrene-butadiene ABA block copolymers, the 4-vinylbiphenyl-isoprene ABA block copolymer exhibits useful mechanical properties below 20 weight percent of vinylaromatic segment. The copolymers could not be compression molded but could be solution cast.

RECEIVED JAN 10 1966

Diffusion and permeation studies were carried out to see whether changes in morphology in the block copolymer would affect the permeation and diffusion rates. To carry out these studies, some time was devoted to evolving a new and greatly improved apparatus. Because of the potential commercial importance of this instrument, its development was also funded by Stanford Research Institute and by the Dohrman Instrument Company which has acquired commercial rights to the instrument and is now manufacturing it.

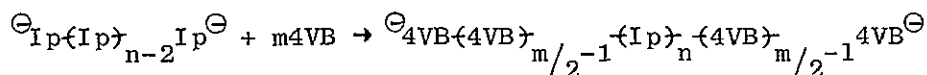
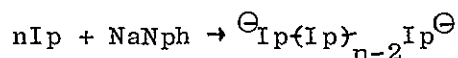
The morphology of block copolymers has been varied by casting films from different solvents. Diffusion and permeation data using carbon dioxide, oxygen, and nitrogen as permeants showed no correlation with morphology.

III DISCUSSION

1 Preliminary Considerations

The primary prerequisite to the synthesis of pure block copolymers is rigorous purity of the monomers. Isoprene is relatively easy to purify to a very high degree by distillation from sodium mirrors,¹ but the solid nature of 4-vinylbiphenyl makes its rigorous purification very difficult.

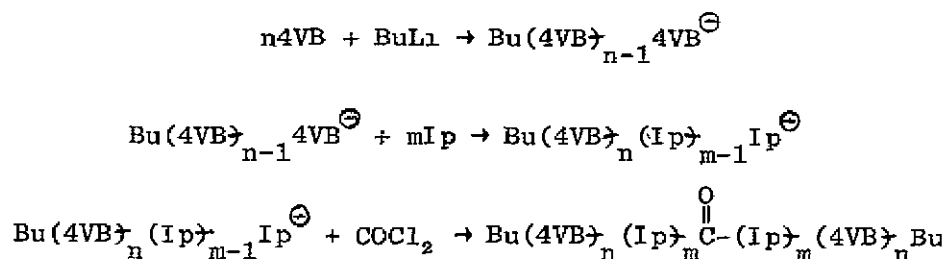
Initial attempts to prepare ABA block copolymers, where A represents a poly-2-vinylnaphthalene or poly-4-vinylbiphenyl segment and B represents a polyisoprene segment, consisted of the preparation of a polyisoprene difunctional anion in tetrahydrofuran, using sodium naphthalene initiation, and then adding carefully purified vinylaromatic monomer to the reaction mixture.



Ip = isoprene, 4VB = 4-vinylbiphenyl, NaNph = sodium naphthalene

However, despite the great deal of work that was devoted to working out methods capable of yielding rigorously pure vinylaromatic monomers, the level of purity was never sufficiently high to permit the synthesis of acceptable materials. Furthermore, preliminary evaluation of some of the better materials at the Jet Propulsion Laboratory indicated that the predominantly 1,2 and 3,4 microstructure of the polyisoprene segment, which is obtained when the polymerizations are carried out in tetrahydrofuran, leads to materials that have an undesirably high middle segment glass transition temperature.

It was therefore decided to change our experimental procedure and to use n-butyllithium initiation in benzene solvent. This procedure not only leads to a pure 1,4-microstructure for the polyisoprene which has a very low glass transition temperature, but also eliminates the necessity for a rigorously pure vinylaromatic monomer. The approach consists of initiating the polymerization of the vinylaromatic monomer with n-butyllithium in benzene, allowing the polymerization to go to completion, adding isoprene to the monofunctional polyvinylaromatic anion, and adding a reactive dihalide to couple the AB anion to an ABBA block copolymer



BuLi = n-butyllithium

Using this approach the residual impurities in the vinylaromatic monomer do not lead to homopolymer contamination but merely destroy some of the n-butyllithium initiator, this is reflected only in the molecular weight of the polyvinylaromatic segment that is higher than calculated. By estimating the degree of purity, it is not difficult to use a slight excess of n-butyllithium and thus compensate for the amount of initiator that is destroyed.

2 Coupling Studies

A key step in this procedure is the coupling of two AB segments with a reactive dihalide. Although a number of investigators mention the coupling of polymeric anions with reactive dihalides,² there are no experimental details nor satisfactory descriptions of experimental results available in the literature. We have therefore, reinvestigated the coupling of a polyisoprene anion with various dihalides. Results of this study are summarized in Table I.

Table I

COUPLING OF POLYISOPRENE ANIONS (Pip) WITH REACTIVE DIHALIDES

Run No	Conditions	Percent Coupled
8430-66	$(\text{CH}_3)_2\text{SiCl}_2$ at 25°C , fast	0
8871-4	$\text{Br}(\text{CH}_2)_4\text{Br}$ at 25°C fast	0
8871-7-1	COCl_2 at -70°C to 25°C , fast, Pip at 25°C	~ 30
8871-7-2	COCl_2 at -70°C to 25°C , slowly, Pip at 40°C	~ 48
8871-7-3	COCl_2 at -70°C to 25°C , slowly, Pip at 0°C	~ 43
8871-7-4	COCl_2 at -70°C to 0°C , slowly, Pip at 0°C	~ 58
8871-8	Approx stoichiometric ammount of COCl_2 added through a capillary	> 90

The degree of coupling was determined from integrated gel permeation chromatography (GPC) areas. Figure 1 shows GPC traces corresponding to various degrees of coupling.

The negative results of the first two experiments (8340-66 and 8871-4) were due to failure to add the coupling agent very slowly. The importance of this very slow addition is shown by the remaining runs which utilized phosgene. It should be noted that when a fast addition was used, only 30 percent coupling was obtained and that various other attempts without special refinements of experimental technique led to only about 50 percent coupling. However, when an approximately stoichiometric amount of phosgene was added through a specially constructed capillary having an extremely small orifice (8871-8), almost quantitative coupling was achieved. The construction of the phosgene tube is shown in Fig. 2.

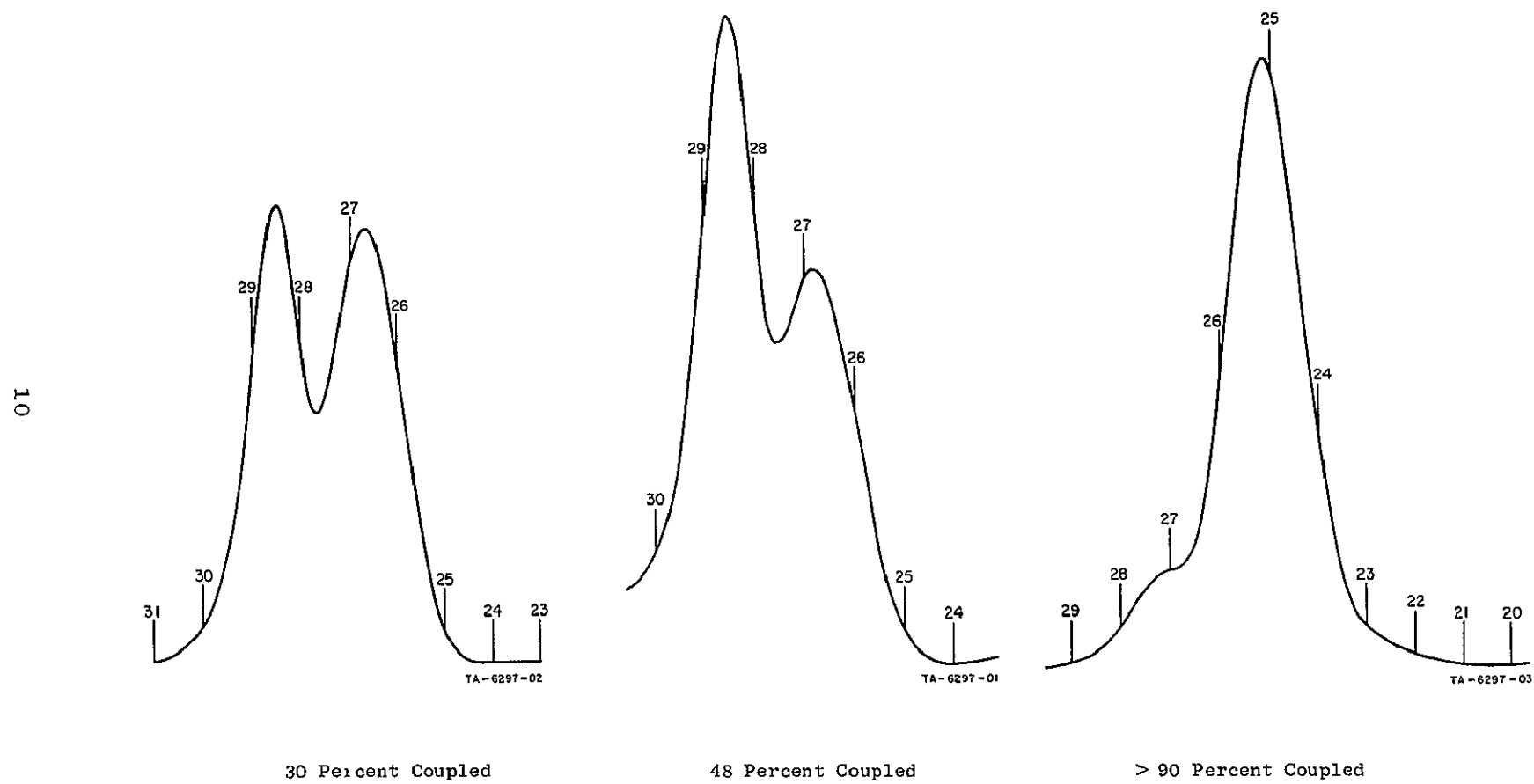


FIGURE 1 GPC OF COUPLED POLYISOPRENE SEGMENTS

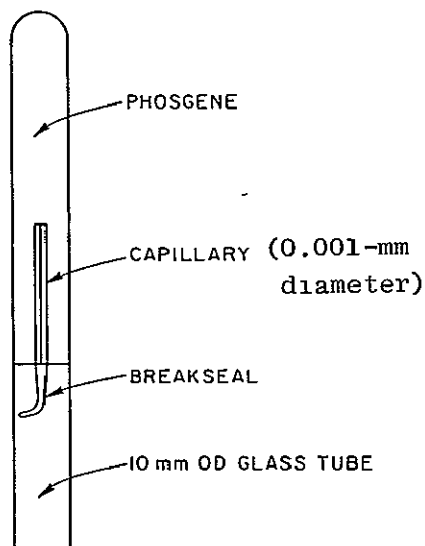


FIGURE 2 CONSTRUCTION OF PHOSGENE TUBE

3 Block Copolymer Synthesis

Results of preliminary syntheses of AB or BA segments are shown in Table II. In these experiments, B represented polyisoprene and A either poly-2-vinylnaphthalene or poly-4-vinylbiphenyl. These experiments were important because some early runs had suggested that a polyvinylaromatic anion would not cleanly initiate the polymerization of isoprene. However, the experimental results established clearly that AB or BA block copolymers can be easily prepared. It was also found from these and subsequent runs that 4-vinylbiphenyl is somewhat easier to purify than 2-vinylnaphthalene, so work with 2-vinylnaphthalene has been discontinued.

Table III shows selected runs where AB segments were coupled with phosgene. As can be seen, A and AB segments of predictable molecular weight could be prepared in most cases. Also, the degree of coupling was reasonably high.

Table II
SYNTHESIS OF AB AND BA BLOCK COPOLYMERS

Run No	Type of Polymer ^a	Molecular Weight of Indicated Segment		Molecular Weight of Block		Percent Vinylaromatic in Copolymer ^b
		Calc	Obs	Calc	Obs.	
8430-66	BA	<div style="text-align: center;">B</div> <div style="display: flex; justify-content: space-between;"> 49,000 49,600 </div>		71,000	90,000	30
8430-68	AB	<div style="text-align: center;">A</div> <div style="display: flex; justify-content: space-between;"> 20,600 21,000 </div>		94,000	126,000	22
8430-69	AB	<div style="text-align: center;">A</div> <div style="display: flex; justify-content: space-between;"> 14,000 15,000 </div>		58,000	---	28
8871-3	BA	<div style="text-align: center;">B</div> <div style="display: flex; justify-content: space-between;"> 51,000 36,000 </div>		49,000	---	27
8871-4	BA	<div style="text-align: center;">B</div> <div style="display: flex; justify-content: space-between;"> 43,500 31,000 </div>		42,000	50,500	25

^a A = poly-2-vinylnaphthalene, except in 8430-68, where A = poly-4-vinylbiphenyl
B = polyisoprene

^b By uv spectroscopy

Table III

PREPARATION OF 4-VINYLBIPHENYL ISOPRENE BLOCK COPOLYMERS

Run No	Molecular Weight Poly-4-vinylbiphenyl		Molecular Weight AB Segment		Percent Coupled	% 4VB in Block Copolymer	Polymer Structure (mol wt $\times 10^{-3}$)
	Calc	Obs	Calc	Obs			
8871-15	4,300	4,200 ^a	55,000	56,000 ^b	100	7.5	4 2 -104- 4 2
8871-16	8,000	10,400 ^a	73,000	69,000 ^b	88	15 0	10.4 -116- 10 4
8871-21	20,000	20,000 ^a	90,000	110,000 ^a	70	31.0	20.0 -140- 20 0
8871-22	15,000	16,000 ^a	76,000	76,000 ^a	93	20 0	16 0 -120- 16.0
8871-24	19,500	28,000 ^b	74,000	90,000 ^a	87	35.0	28.0 -120- 28 0
8871-26	15,000	25,000 ^a	130,000	128,000 ^b	87	18 0	25 0 -200- 25 0
8871-27	9,000	9,000 ^a	66,000	65,000 ^b	89	15 0	9 0 -112- 9 0
8871-30	4,500	4,500 ^a	53,500	56,000 ^b	95	8 0	4 5 -101- 4 5

^a By GPC^b By osmometry

4. Polymer Characterization

A particularly attractive aspect of preparing ABA block copolymers by a coupling technique is that the molecular weight of the ABA block is double that of the AB segment so that gel permeation chromatography (GPC) can easily resolve the polymer components. This is not always possible with polymers prepared by sequential addition, particularly materials that have an A segment of relatively low molecular weight.

Since GPC uses a differential refractometer as a detector, the peak area is proportional to the amount of sample eluted and to the refractive index increment. If the ratio of refractive index increments of the two homopolymers and the overall composition of the injected material are known, the constituent polymers in the sample can be quantitatively determined.

The overall composition of the sample can be calculated from the monomer feed, provided the conversion is quantitative, but it is better determined from the ultraviolet maximum of 4-vinylbiphenyl at 2575 Å, using a calibration plot shown in Fig. 3.

Figure 4 shows a plot of refractive index increments ($\Delta n/C = n$) at 5460 Å of various 4-vinylbiphenyl-isoprene block copolymers versus the weight fraction of poly-4-vinylbiphenyl. The linearity of the plot verifies that the contributions of the two homogeneous segments to the overall refractive index are additive.

In view of the linear relationship, the refractive index increment of the polymer can be expressed as follows:

$$n_{A+B} = \dot{n}_B + W_A (n_A - n_B) \quad (1)$$

where \dot{n}_A and n_B are the refractive index increments of homopolymers A and B, and W_A is the weight fraction of A in the sample. If the GPC trace shows a single peak of area "a" corresponding to homopolymer A and a single or double peak of total area "b" for the block (ABBA and/or AB), then the following relationships will hold:

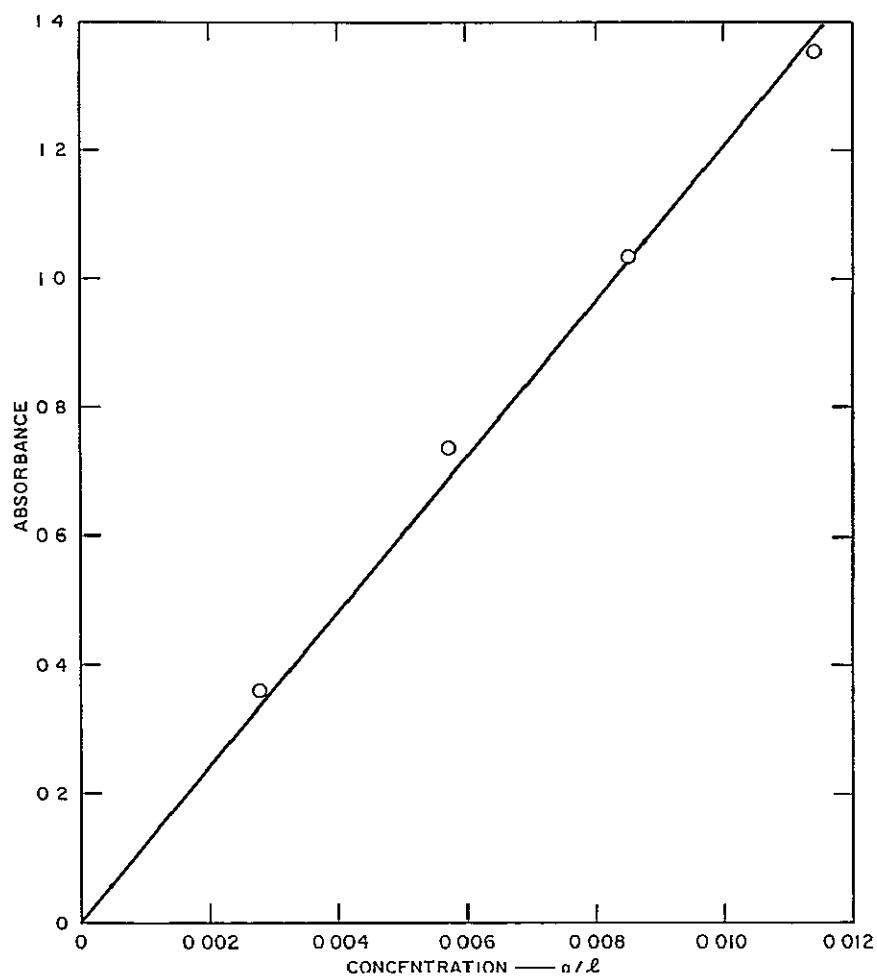


FIGURE 3 ULTRAVIOLET ABSORPTION AT 2575 Å OF POLY-4-VINYLBIPHENYL IN TETRAHYDROFURAN AS A FUNCTION OF CONCENTRATION

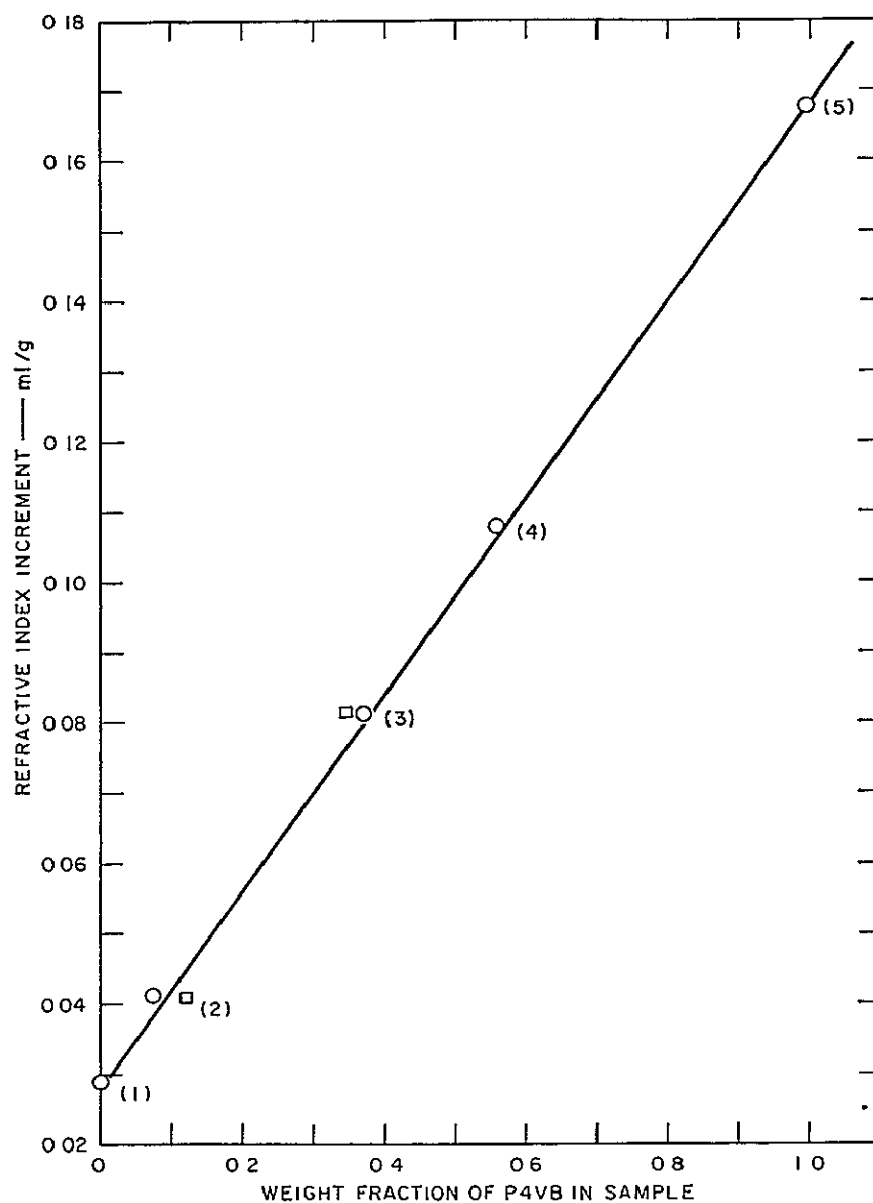


FIGURE 4 REFRACTIVE INDEX INCREMENT IN TOLUENE OF 4-VINYLBIPHENYL (a) ISOPRENE (b) BLOCK COPOLYMERS AS A FUNCTION OF WEIGHT FRACTION OF 4-VINYLBIPHENYL Samples and molecular weights are (1) B (91,000), (2) ABBA (117,000), (3) AB (97,000), (4) AB (97,000) + ABA (124,000), (5) A (130,000), weight fraction A calculated from (O) weight or (□) ultraviolet data

$$w_A^a = k(a/n_A) \quad (2a)$$

$$w_{AB}^b = k(b/n_{AB}) \quad (2b)$$

$$w_A^a + w_{AB}^b = 1 = k(a+b)/n_{A+B} \quad (2c)$$

where w_A^a and w_{AB}^b are the weight fractions associated with the peak areas, k is a proportionality factor, and n_{A+B} is the refractive index increment of the injected sample

By dividing (2a) by (2c) and substituting Eq (1) for n_{A+B} one obtains

$$w_A^a = a/(a+b)(n_{A+B}/n_A) = a/(a+b) [(n_B/n_A) + w_A(1-n_B/n_A)] \quad (3)$$

The weight fraction of A in the original material w_A can be determined, as already mentioned, from the ultraviolet spectrum, and the ratio n_B/n_A can be determined with a differential refractometer. Alternatively, a solution of known composition can be injected in a GPC unit, and, provided the two peaks are clearly resolved, n_B/n_A can be evaluated as follows.

$$n_B/n_A = a_B w_A / a_A w_B \quad (4)$$

where a_1 and w_1 represent the respective peak areas and homopolymer weights

Thus, with a knowledge of w_A and n_B/n_A , w_A^a can be calculated from Eq (3) and the weight fraction w_{AB}^b can be determined by simple arithmetic. Since in the case treated here the composition of AB and ABBA is the same, their relative amounts are equal to the respective areas

$$w_{AB}^b = w_{AB}^{tot} [b_1/(b_1+b_2)] \quad (5a)$$

$$w_{ABBA}^b = w_{AB}^{tot} [b_2/(b_1+b_2)] \quad (5b)$$

where b_1 and b_2 are the respective GPC areas of the AB and ABBA segments

The results of a few representative runs analyzed by the GPC procedure described are shown in Table IV

Table IV
CHARACTERIZATION OF 4-VINYLBIPHENYL-ISOPRENE ABBA BLOCK COPOLYMERS

Run No	Molecular Weight		Weight Fraction of A, W_A^\ddagger	Composition of Block ^{**}		
	Total [*]	A Segment [†]		W_A^a	$W_{AB}^{b_1}$	$W_{ABBA}^{b_2}$
8871-13	280,000	69,000	0.450	0.047	0.260	0.690
8871-15	112,000	4,000	0.075	0	0	1.000
8871-16	138,000	10,000	0.150	0.020	0.130	0.850

* By membrane osmometry.

† From Eq (1) and ultraviolet composition as follows $\bar{M}_n(A) = \frac{\%4VB \times \bar{M}_n \text{ total}}{2}$

‡ From ultraviolet at 2575 Å

** From GPC

Figures 5, 6 and 7 show gel permeation chromatograms of the A segment, the AB segment, and the final ABBA polymer. These chromatograms clearly show that narrow molecular weight distribution poly-4-vinylbiphenyl segments can be produced in benzene without the necessity of adding ethers (Fig. 5) and that these cleanly initiate the polymerization of isoprene to produce a narrow molecular weight distribution AB segment (Fig. 6). It is also clear that the purity of the isoprene monomer is very high and that only a very small amount of the poly-4-vinylbiphenyl anion is killed. That this small peak at count 28 (Fig. 6) is dead poly-4-vinylbiphenyl and not unreacted live poly-4-vinylbiphenyl can be proved by the results shown in Fig. 7, where no movement of this peak to higher molecular weight is noted after addition of phosgene.

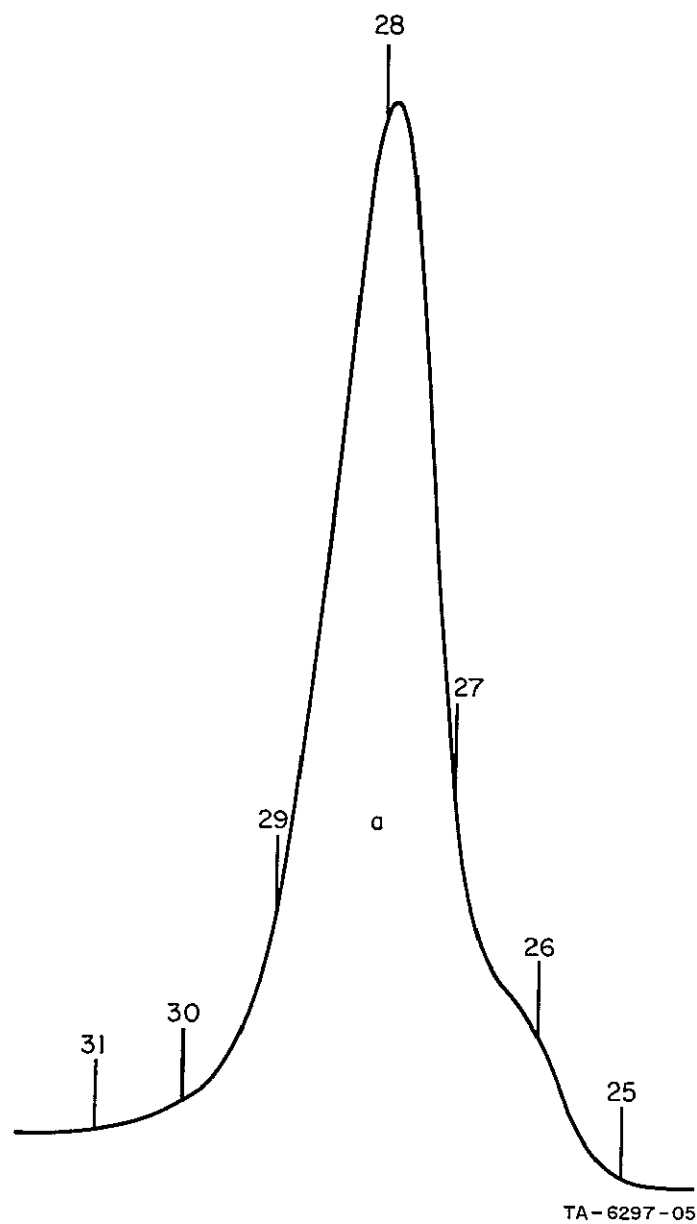


FIG 5 POLY-4-VINYLBIPHENYL A SEGMENT, RUN 8871-13

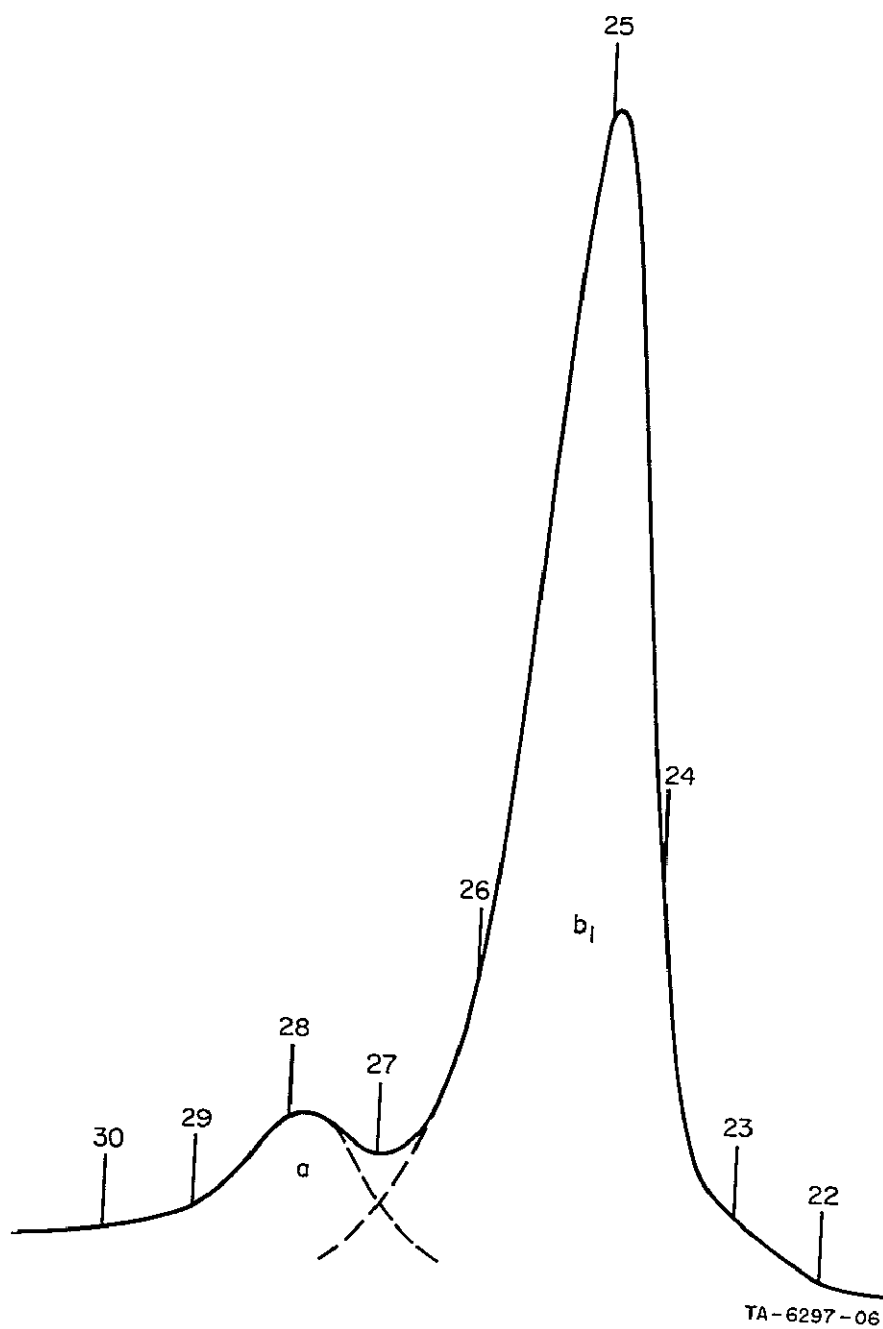


FIG 6 POLY-4-VINYLBIPHENYL-POLYISOPRENE AB SEGMENT, RUN 8871-13

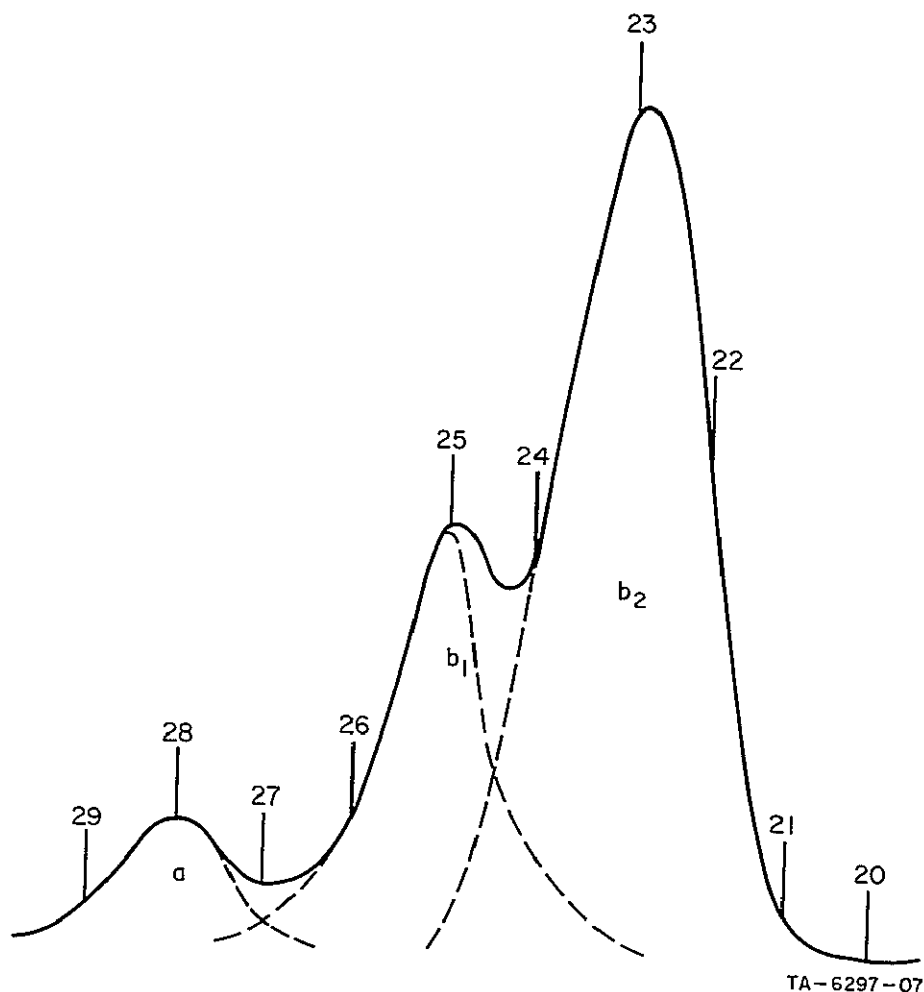


FIG 7 POLY-4-VINYLBIPHENYL-POLYISOPRENE ABBA BLOCK COPOLYMER
(75% Coupled, <5% Homopolymer), RUN 8871-13

5 Mechanical Properties

Many attempts were made to fabricate specimens suitable for mechanical testing. It was not possible to obtain good specimens by compression molding or injection molding because, at the high temperatures necessary to mold poly-4-vinylbiphenyl, considerable decomposition of the polyisoprene took place. Thus, these attempts were discontinued, and films were cast from a 90/10 tetrahydrofuran/methyl ethyl ketone solution. Rings were then cut from the cast sheets and tested on an Instron tester. Typical results of these measurements are shown in Table V.

These are interesting results since they show that, unlike a styrene-isoprene ABA block copolymer, the 4-vinylbiphenyl-isoprene ABA block copolymer exhibits useful mechanical properties below 20 weight percent of vinylaromatic segment.

Table V

STRESS-STRAIN PROPERTIES OF PVB-PIP-PVB BLOCKS

Run No	σ_b kg/cm ²	$\sigma_{\lambda=4}$ kg/cm ²	λ_b	Wt Percent of 4-Vinylbiphenyl
8871-24-3	250	62	11.3	35
8871-26-3	165	18	15.5	18
8871-27-3	106	12	18.5	15
8871-30-3	50	8	16.5	8

6 Permeation and Diffusion Studies

Initial studies have been carried out of the effect of morphology on diffusion rates of hydrazine and n-hexane through a 4-vinylbiphenyl-isoprene-4-vinylbiphenyl block copolymer, using a rather crude apparatus. A standard O-ring joint was set up with a membrane clamped between the O-ring and the glass groove. The clamped joint was then placed in an upright position, and hydrazine or n-hexane was poured on top of the membrane. The bottom joint was connected to a small capillary which was cooled in liquid nitrogen. Periodically, the capillary was disconnected, a standard amount of toluene was added, and an aliquot was analyzed by glc. Preliminary results of n-hexane diffusion measurements through a copolymer having 50% 4-vinylbiphenyl content were as follows: film cast from 90/10 tetrahydrofuran/methyl ethyl ketone had a diffusion rate of 1600 g-mil/m²-24 hr, film cast from carbon tetrachloride had a diffusion rate of 3350 g-mil/m²-24 hr. These numbers are, however, only of qualitative significance, since gaseous diffusion of the permeant through the capillary was found to be the rate determining step for the condensation. Nevertheless, these results provide initial verification of the hypothesis that diffusion rates can be modified by changes in morphology. No measurable amounts of hydrazine were condensed.

This experimental method, however, was inaccurate, and the results were irreproducible. We decided to evolve an experimental technique that could routinely yield accurate and reproducible data on permeation and diffusion rates. In brief, a prototype instrument, which is basically a gas chromatograph, has been developed in which the column has been replaced by the permeation cell. The carrier gas (helium) passes through one compartment, and the permeant is introduced into the other. The permeant diffusing across the membrane moves with the carrier gas to the detector. The continuous signal produced is proportional to the permeation rate, if the flow rate is constant and sufficiently high. Since both compartments are at atmospheric pressure, no membrane support is required.

A simple mathematical formalism has also been developed for deriving diffusion coefficients from the measured transition-state permeation rates. Permeation and diffusion coefficients and the respective activation energies have been determined for CO_2 , O_2 , N_2 , and liquid hexane through polyethylene membranes. The results agree closely with literature data.

Because of the potential commercial importance of this instrument, this work was also funded in part by Stanford Research Institute and by the Dohrman Instrument Company which has acquired commercial rights to the Instrument and is now manufacturing it under the name "Polymer Permeation Analyzer."

A detailed account of the method and apparatus has been published in the Journal of Polymer Science. The paper is attached as Appendix A.

Because of the availability of substantial amounts of pure and well characterized styrene-butadiene ABA block copolymers from the Shell Chemical Company, a careful study of the effect of morphology on diffusion and permeation rates was carried out using these materials. Table VI lists the characterization data supplied by the Shell Chemical Company.

Table VI
CHARACTERIZATION OF SHELL BLOCK COPOLYMERS

Property	Copolymer		
	TR-41-1467	TR-41-1468	TR-41-1469
Molecular weight, \bar{M}			
\bar{M}_{S1}	9,600	14,500	13,600
\bar{M}_B	47,500	27,900	69,800
\bar{M}_{S2}	9,400	13,700	14,500
Total molecular weight, \bar{M}_T	66,500	56,100	97,900
Ratio, $\frac{\bar{M}_B}{\bar{M}_{S1} + \bar{M}_{S2}}$	2.50	0.99	2.48

In addition GPC analyses were carried out in trichloroethylene solvent with the following results

Copolymer	GPC Count (% total area)
TR-41-1467	27.3 (90%), 38.5 (10%)
TR-41-1468	27.2 (90%), 38.4 (10%)
TR-41-1469	26.0 (95%), 38.5 (5%)

The peak at count 38.5 represents a low molecular weight impurity.

Films from the copolymers were cast from two different solvents that are known to produce different morphological structures³. Thus, films cast from 90/10 benzene/heptane show discrete polystyrene domains, but films cast from carbon tetrachloride show diffuse phase boundaries between the styrene and butadiene phases.

Results of diffusion studies with carbon dioxide, oxygen, and nitrogen are shown in Tables VII and VIII. Examination of the data shows that

Table VII

PREPARATION AND PERMEATION DATA FOR THIN FILMS OF
SBS BLOCK COPOLYMERS CAST FROM 90/10 BENZENE/HEPTANE

Copolymer Sample	Preparation Data		Diffusion and Permeation Data *						
	Drying Conditions	Thickness (mils)	Permeant	D_{25} (cm^2/sec)	D_0 (cm^2/sec)	E_D (kcal/mole)	P_{25} (cm/sec)	P_0 (cm/sec)	E_P (kcal/mole)
TR-41-1467-4LT	Dried in vacuo (R T \dagger /114 hours)	5.65-5.90	CO ₂	1.47×10^{-6}	1.92×10^{-2}	5.61	2.34×10^{-8}	1.58×10^{-5}	3.85
			O ₂	2.03×10^{-6}	1.5×10^{-2}	5.27	3.45×10^{-9}	5.29×10^{-5}	5.70
			N ₂	1.66×10^{-6}	3.2×10^{-2}	5.84	1.39×10^{-9}	6.55×10^{-5}	6.37
TR-41-1468-4LT	Dried in vacuo (R T /117 hours)	6.3-6.6	CO ₂	4.68×10^{-7}	1.23×10^{-2}	6.03	7.8×10^{-9}	6.64×10^{-6}	3.99
			O ₂	8.0×10^{-7}	6.4×10^{-3}	5.32	1.25×10^{-9}	2.91×10^{-5}	5.96
			N ₂	4.48×10^{-7}	3.3×10^{-2}	6.63	4.01×10^{-10}	5.85×10^{-5}	7.04
TR-41-1469-4LT	Dried in vacuo (R T /141 hours)	5.5-5.9	CO ₂	1.49×10^{-6}	1.3×10^{-3}	4.0	2.50×10^{-8}	7.36×10^{-6}	3.36
			O ₂	2.09×10^{-6}	8.25×10^{-4}	3.54	3.69×10^{-9}	5.3×10^{-5}	5.67
			N ₂	1.50×10^{-6}	3.0×10^{-3}	4.51	1.42×10^{-9}	7.40×10^{-5}	6.42

* D_{25} = diffusion coefficient at 25°C, D_0 = diffusion coefficient at $1/T = 0$, E_D = heat of diffusion,

P_{25} = permeation coefficient at 25°C, P_0 = permeation coefficient at $1/T = 0$, E_P = heat of permeation

\dagger R T = room temperature

Table VIII

PREPARATION AND PERMEATION DATA FOR THIN FILMS OF
SBS BLOCK COPOLYMERS CAST FROM CCl_4

Copolymer Sample	Preparation Data		Diffusion and Permeation Data*						
	Drying Conditions	Thickness (mils)	Permeant	D_{25} (cm^2/sec)	D_0 (cm^2/sec)	E_D (kcal/mole)	P_{25} (cm/sec)	P_0 (cm/sec)	E_P (kcal/mole)
TR-41-1467- 5LT	Dried in vacuo ($R T \uparrow/120$ hours)	5 20-5 25	CO_2	1.40×10^{-6}	5.3×10^{-3}	4.91	2.24×10^{-8}	8.92×10^{-6}	3.55
			O_2	1.75×10^{-6}	9.6×10^{-3}	5.10	3.29×10^{-9}	6.56×10^{-5}	5.86
			N_2	1.63×10^{-6}	4×10^{-3}	4.61	1.28×10^{-9}	1.00×10^{-4}	6.67
TR-41-1468- 5LT	Dried in vacuo ($R T /161$ hours)	5 20-5 30	CO_2	5.12×10^{-7}	4.0×10^{-3}	5.30	8.90×10^{-9}	6.55×10^{-6}	3.91
			O_2	8.40×10^{-7}	1.02×10^{-2}	5.57	1.37×10^{-9}	3.16×10^{-5}	5.95
			N_2	5.26×10^{-7}	7.7×10^{-2}	7.04	4.60×10^{-10}	6.54×10^{-5}	7.02
TR-41-1469- 5LT	Dried in vacuo ($R T /162$ hours)	5 7 -5 8	CO_2	1.14×10^{-6}	6.8×10^{-3}	5.15	2.38×10^{-8}	5.5×10^{-6}	3.22
			O_2	1.64×10^{-6}	1.3×10^{-3}	3.94	3.67×10^{-9}	4.56×10^{-5}	5.58
			N_2	1.38×10^{-6}	2.6×10^{-3}	4.46	1.47×10^{-9}	6.68×10^{-5}	6.35

* D_{25} = diffusion coefficient at 25°C , D_0 = diffusion coefficient at $1/T = 0$, E_D = heat of diffusion

P_{25} = permeation coefficient at 25°C , P_0 = permeation coefficient at $1/T = 0$, E_P = heat of permeation

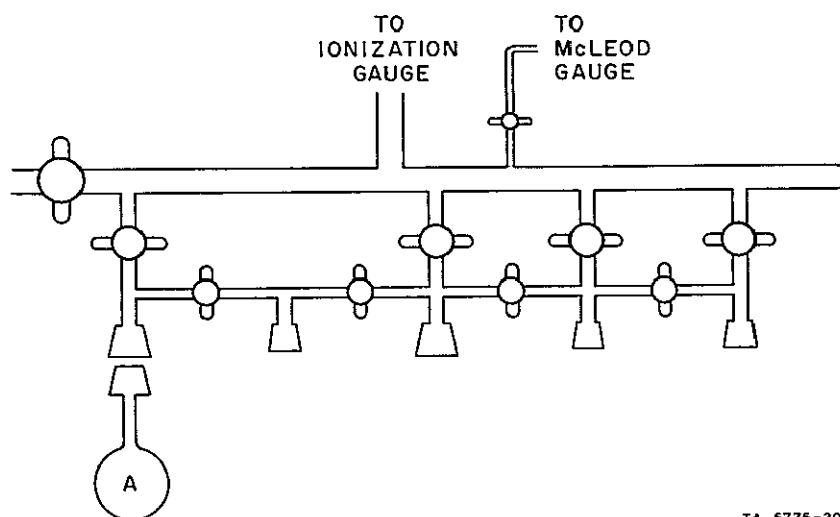
$\uparrow R T$ = room temperature

the values of D_{25} , P_{25} , and P_0 for copolymers 1467 and 1469 are approximately the same order of magnitude for corresponding permeants, even though the total molecular weight of each copolymer is quite different. The ratio of butadiene/styrene, however, is practically the same for each. Only the value of P_0 seems to decrease by about a factor of 10 (for CO_2 and N_2). Thus, morphological differences are not reflected in the permeation and diffusion data obtained for the two sets of films. The differences between corresponding values in Tables VII and VIII are not significant since, in general, each pair of values lies within the experimental error of the measurements. However, the choice of permeants may not have been the best, and a permeant that is very soluble in one phase and insoluble in the other may well have shown differences that could be correlated with morphological features.

IV EXPERIMENTAL

1 Apparatus

Polymerizations were carried out on the vacuum system shown in Fig. 8. It consists of a manifold of 30-mm OD tubing, 28 in. long, which could be routinely evacuated to 10^{-5} torr by means of a Duo-Seal mechanical fore-pump and a mercury diffusion pump. Bulb A (1000 ml) was used for storage of purified benzene which was kept over polystyryl lithium as scavenger. The red color of the solution was taken as evidence of purity. Early experiments used tetrahydrofuran which was kept over sodium naphthalene



TA-5775-20R

FIGURE 8 SCHEMATIC DIAGRAM OF VACUUM SYSTEM

2 Purification of Materials

a Isoprene

The monomer (Phillips Petroleum, Research Grade) was placed over calcium hydride on a vacuum system, degassed, and allowed to stand for 24 hr. It was then distilled into a bulb containing a sodium mirror, allowed to react for 2-3 hr, distilled into another bulb with a sodium mirror, allowed

to react again for 2-3 hr, and finally distilled into a tube with a break-seal. This tube was stored in a freezer until ready for use.

b 4-Vinylbiphenyl

The monomer (Aldrich Chemical Company) was first dissolved in benzene and passed through a column containing successive layers of silicic acid and alumina. It was then recrystallized to a sharp melting point from methanol and dried. The monomer was next dissolved in pure benzene to a known concentration, and a measured amount of this solution was injected through a neoprene serum cap (A) into bulb B, which contained calcium hydride (Fig. 9). Next, the solution in bulb B was frozen, the apparatus

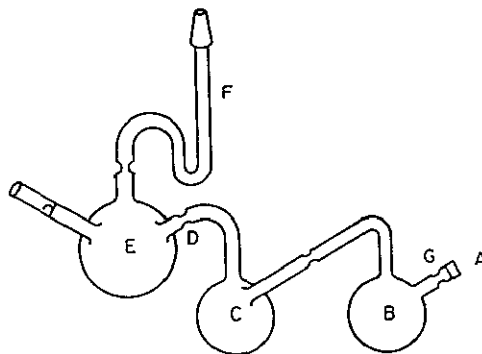


FIGURE 9 APPARATUS FOR PURIFICATION OF 4-VINYLBIPHENYL

evacuated, and the tube sealed off at G. The mixture was allowed to melt and then left standing at room temperature until all evolution of hydrogen ceased (about 18 hrs). The solvent was stripped off and the monomer carefully sublimed into bulb C. Bulb B was then sealed off and the monomer sublimed into bulb E. After sealing off at D, purified benzene was distilled into the bulb, and the contents were frozen and degassed. The bulb was then sealed off at F and stored in a freezer until ready for use.

c. Sodium Naphthalene

Sodium naphthalene was prepared using the apparatus shown in Fig 10. Sodium metal was placed in tube C, and a mirror was formed in bulb B. Tube C was then sealed off at D. Sublimed naphthalene was placed in bulb A, tetrahydrofuran was distilled into bulb A, and the apparatus sealed off at E. The tetrahydrofuran solution of naphthalene was then poured into bulb B and allowed to react for 24 hrs. The resulting green solution was poured back into bulb A through the sintered glass filter, sealed off at F, and distributed into ampules equipped with breakseals through G. They were stored in a freezer.

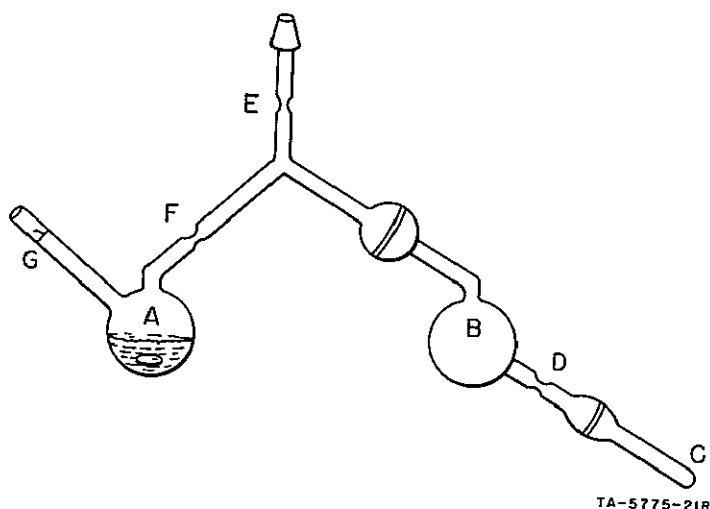


FIGURE 10 REACTOR FOR PREPARATION OF SODIUM NAPHTHALENE

d. Butyllithium

Using a hypodermic syringe, n-butyllithium initiator was taken directly from the bottle (Foote Mineral Co, 1.6 M in n-hexane) and transferred in an argon-filled polyethylene bag into a tube equipped with a breakseal at one end and a constriction and a neoprene serum cap on the other end. The contents of the tube were frozen in liquid nitrogen, the tube evacuated through a syringe needle, the contents allowed to melt, and again frozen and evacuated. The tube was next sealed off at the constriction and was ready for use.

Phosgene gas used in the coupling experiments was admitted up to atmospheric pressure in a vacuum system into a small bulb equipped with a breakseal and a capillary tube having an extremely small orifice. The phosgene was liquified and the tube sealed off. The volume was calculated so that a slight excess over the stoichiometric amount was available for the coupling reaction.

3 Block Copolymer Synthesis

Polymerizations were carried out in the apparatus shown in Figure 11. An initiator bulb E, an isoprene bulb F, a 4-vinylbiphenyl benzene solution bulb G, and a phosgene bulb H were sealed onto the reactor B. The whole assembly was then evacuated to 10^{-5} torr and flamed. After cooling the assembly, benzene was condensed into bulb B and degassed, and the reactor was sealed off at A. The initiator ampoule E was broken and the whole apparatus thoroughly rinsed with the benzene-initiator solution. The 4-vinylbiphenyl bulb G was next broken and the polymerization allowed to proceed about 4-5 hr, during which time the solution gradually developed a deep red color. A portion of the solution in B was then transferred

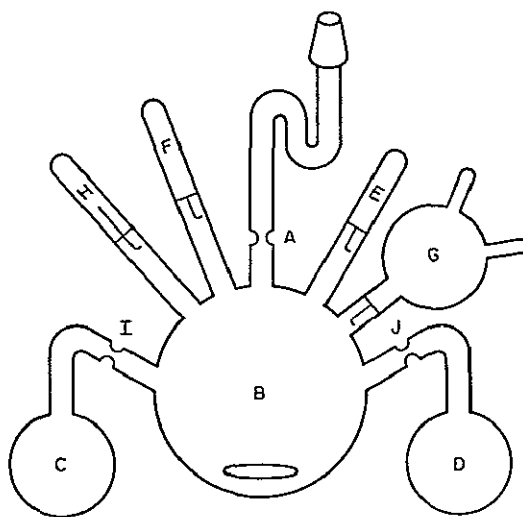


FIGURE 11 POLYMERIZATION APPARATUS

to bulb C which was sealed off at I. Then the isoprene ampule F was broken. Depending on the relative amounts of isoprene and 4-vinylbiphenyl, the color changed either abruptly or gradually to yellow. The polymerization was usually allowed to proceed overnight, and a portion of this solution was then transferred to bulb D, which is sealed off at J. The phosgene ampule H was next broken, and the gas was allowed to diffuse very slowly into the polymer solution which was vigorously agitated until the solution became colorless. The reactor was opened, the material was poured into an excess of methanol, and based on the amount of polymer, about 1% of β -phenylnaphthylamine antioxidant was added. The coagulated polymer was filtered and dried overnight in a vacuum oven. The contents of bulbs C and D were also worked up and the contents used for characterization of the A and AB segments.

4. Polymer Characterization

The block copolymers were characterized by gel permeation chromatography (GPC) and osmometry. Gel permeation chromatography measurements were carried out on a Waters Associates unit using a combination of four columns filled with a crosslinked polystyrene gel having the following pore sizes: one 1×10^6 , one 1.5×10^5 , one 3×10^4 , and one 8×10^3 Å. The operating conditions were toluene solvent at 70°C, pumped at 1 cc/min. Number-average molecular weight measurements were determined on a Mechrolab high-speed osmometer, and differential refractive indices were measured with a Brice-Phoenix instrument.

5. Mechanical Property Measurements

a. Film Casting

The block copolymer was dissolved in a 90/10 tetrahydrofuran/methyl ethyl ketone solution to a concentration of 20 percent. A glass ring was then placed on a thin Teflon sheet stretched tightly across a glass plate and the polymer solution was poured into the ring to a depth of 1 mm. The solvent was allowed to evaporate and then the polymer film was dried to constant weight in a vacuum oven. Sheets 0.25 mm thick were obtained by this procedure.

b Stress-Strain Data

Rings having an outside diameter of 20 mm and an inside diameter of 13 mm were punched from the films and tested on a Instron tester at room temperature and crosshead speed of 2 in /min.

6 Diffusion Studies

a Film Casting

All films were cast from a 15% (w/v) solution of the block copolymer in the appropriate solvent using a 0.030-in. doctor blade. The solvent was allowed to evaporate slowly at room temperature for one hour before the film was dried in a vacuum oven. Thin films of polystyrene were also prepared to serve as a basis of comparison in the permeation study.

b Permeation Studies

A complete description of the apparatus and procedure is found in the copy of the manuscript attached as Appendix A.

REFERENCES

- 1 M. A. Morton, E E Bostick, and R G Clarke, J Polym Sci., A, 1, 475 (1963)
- 2 J A Gervasi and A B Gosnell, J. Polym. Sci , A-1, 4, 1391 (1966)
- 3 J F. Beecher, L Marker, R D Bradford, and S. L Aggarwal, J Polym Sci , C, 26, 117 (1969)

PHASE II

I INTRODUCTION

The objective of this phase was the preparation of ABA block copolymers that do not contain C-H bonds and that would thus be expected to yield elastomers resistant to strong oxidants

II SUMMARY

Initial attempts to prepare ABA block copolymers that did not contain C-H bonds were based on the anionic polymerization of α,β,β -trifluorostyrene or octafluorostyrene. However, contrary to a literature report, α,β,β -trifluorostyrene could not be polymerized anionically, and this approach was abandoned

A subsequent attempt involved the free radical polymerization of α,β,β -trifluorostyrene in the presence of a chain-transfer agent bis(4-aminophenyl)disulfide, which should produce an amino-terminated polymer. This polymer would then be chain-extended with a difunctional perfluoropropylene oxide to yield an alternating block copolymer. It was, however, not possible to chain-extend the difunctional polystyrene even with simple diisocyanates or diacid chlorides

Block copolymers of polychlorotrifluoroethylene and nitroso rubber were developed by cleaving nitroso rubber with ultraviolet or γ -rays and using the macroradicals as initiators for the polymerization of chlorotrifluoroethylene. This method did indeed produce block copolymers, and a fractionation procedure was worked out whereby pure block copolymers could be isolated from the reaction mixture. The block copolymers had poor mechanical properties because of an insufficient number of cleavages of the nitroso rubber chain or incorrect composition, or both

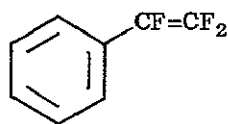
III DISCUSSION

A α,β,β -Trifluorostyrene

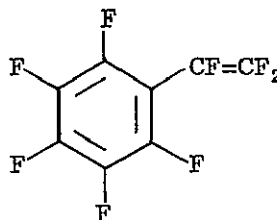
1 Anionic Polymerization

Although the difficulty of anionically polymerizing fluorinated monomers is not to be underestimated, careful consideration of the literature indicated that a number of routes deserved attention

A prime candidate for the high melting A-block is α,β,β -trifluorostyrene (I) or the fully fluorinated compound octafluorostyrene (II)



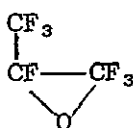
I



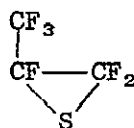
II

Since octafluorostyrene is not commercially available, we decided to initiate this study by investigating the feasibility of carrying out an ionic polymerization of α,β,β -trifluorostyrene (I), which is commercially available.

Expectation that α,β,β -trifluorostyrene could be polymerized anionically was provided by a literature reference¹ that reported the polymerization of this monomer with sodium methoxide, sodium in liquid ammonia, or sodium but gave no experimental details. Should it be possible to prepare living polymers from α,β,β -trifluorostyrene, candidate monomers that could be considered for a flexible middle segment would be perfluoroethers or perfluorothioethers. There have been reports of anionic² and cationic³ polymerization of partially fluorinated oxides, and the polymerization of monomers such as perfluoropropylene oxide (III) or perfluoropropylene sulfide (IV) by these same mechanisms might be possible.



III



IV

If this approach were successful, fully fluorinated AB-type block copolymers consisting of a hard segment and a soft segment would then be available. However, since the anion derived from perfluoropropylene oxide and probably that derived from perfluoropropylene sulfide are even weaker bases than the anion derived from ethylene oxide, which does not initiate the polymerization of styrene,⁴ addition of α,β,β -trifluorostyrene to these living anions would obviously not produce ABA block copolymers. For the same reason, a coupling reaction with methylene dibromide would also fail, although certain very reactive dihalides could possibly serve as coupling agents. A more plausible approach would be to terminate the AB anion with water, thus producing a hydroxyl-terminated AB block copolymer, and to couple two molecules with a diisocyanate.

The anionic polymerizability of α,β,β -trifluorostyrene was screened by using a series of anionic initiators. The results are shown in Table I.

Table I

ATTEMPTS TO ANIONICALLY POLYMERIZE α,β,β -TRIFLUOROSTYRENE AT -50°C

Solvent	Catalyst	Results
Tetrahydrofuran	Aged n-BuLi	No Polymer
Tetrahydrofuran	n-BuLi	No Polymer
Toluene	n-BuLi	No Polymer
Toluene	Na, NaOCH ₃	No Polymer
Dimethylformamide	KF	No Polymer
Dimethylformamide	NaCN	No Polymer
Ammonia	Na	No Polymer

In view of these negative results a new series of polymerization attempts was carried out. In this series, α, β, β -trifluorostyrene was added to various solvent and catalyst systems at -50°C and the temperature then raised to 0°C and 25°C at 20-hr intervals. The amount of unreacted α, β, β -trifluorostyrene in the reaction mixtures was tested by gas liquid chromatography using toluene as an internal standard. At the termination of the runs the reaction mixtures were worked up with isopropanol in an attempt to isolate polymer. None was found, thus corroborating the results shown in Table I.

Measurement of unreacted monomer did, however, show that some catalyst and solvent combinations produced various products that were observed in the gas liquid chromatograms, but no isolation or identification was attempted. Results of this study are shown in Table II.

Table II

ATTEMPTS TO ANIONICALLY POLYMERIZE α, β, β -TRIFLUOROSTYRENE
AT VARIOUS TEMPERATURES

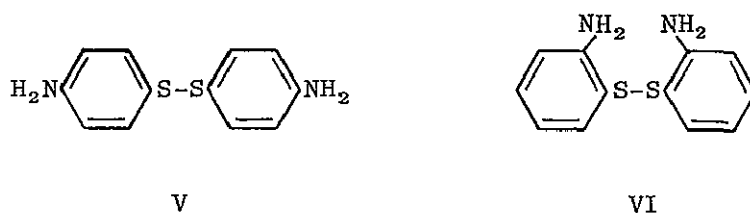
Solvent	Catalyst	Result ^a	
		-50°C	0°C
Methylcyclohexane	Na - sand	N R	R
Methylcyclohexane	NaOMe	N R.	R
Dimethylformamide	NaCN	R	N.C
Tetrahydrofuran	n-BuLi (aged)	N.R.	R
Tetrahydrofuran	n-BuLi (fresh)	R	N C.
Tetrahydrofuran	NaOMe	R	N C
Tetrahydrofuran	Na - sand	Sl R	R

^a R = reaction, N.R. = no reaction, N.C. = no change, Sl R = slight reaction

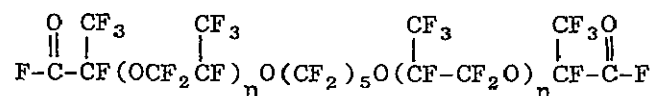
Our continuing inability to anionically polymerize α,β,β -trifluorostyrene has convinced us that further attempts along these lines is of doubtful value and that the literature reference to the anionic polymerization of this monomer is in error. Although it should not be inferred at this point that α,β,β -trifluorostyrene cannot be polymerized anionically, it is very likely that success, if any, could come only by developing novel catalyst systems. Therefore, this approach has been abandoned and free radical techniques were investigated next.

2 Free Radical Polymerization

In this approach the free radical polymerization of α,β,β -trifluorostyrene in the presence of a chain-transfer agent bis(4-aminophenyl)disulfide (V) or bis(2-aminophenyl)disulfide (VI) was carried out.



This polymerization is well worked out for styrene⁵ and should produce a difunctional aminophenyl-terminated poly(α,β,β -trifluorostyrene). The aminophenyl-terminated polymer would then be chain-extended with the known difunctional polymer from perfluoropropylene oxide, obtained by polymerizing this monomer with CsF and glutaryl fluoride, producing the following structure:



Attempts to polymerize TFS in bulk at 50°C or higher yielded little polymer and much dimer.⁶ In the hope of lessening dimerization reactions, bulk polymerization procedures were tried which might proceed at room temperature or below. These included initiation with di(tertbutylperoxy)

oxalate, photochemical initiation by azobisisobutyronitrile (AIBN), and γ -ray initiations. None of these methods gave satisfactory polymerization of TFS (conversions to polymer were < 10%)

Emulsion polymerization was attempted next. The potassium persulfate-initiated polymerizations of TFS in Ivory soap and dodecylamine hydrochloride emulsions gave 48% and 70% conversion to polymer, respectively. However, all persulfate-initiated emulsion polymerizations in the presence of bis(4-aminophenyl)disulfide (V) were unsuccessful.

Successful polymerization of TFS was achieved when the water soluble persulfate initiator was replaced by the organic soluble azobisisobutyronitrile. Conversions to polymer were 40-45% (see Table III). The yield of polymer was not sensitive to wide variation in the level of initiator or the level of bis(4-aminophenyl)disulfide. As the level of disulfide increased, polymer molecular weight decreased and the concentration of end groups increased. The polymers are expected to be difunctional, but the functionality has not been determined. Continuing polymerization longer than 48 hours did not increase the yield of polymer.

Unfortunately, the amino-terminated PTS could not be chain-extended with diisocyanates or diacid chlorides. This can be due to low reactivity of the amino end-group or a consequence of their low concentration, or both. At any rate, our inability to chain-extend the amino-terminated PTS even with simple difunctional compounds does not make this approach very promising, and no further work has been carried out.

B Nitroso Rubber

1 General Considerations

The backbone of nitroso rubber contains -N-O- bonds, which, like -O-O- bonds, are weak and subject to thermal and radiative (γ -ray, uv) cleavage. Associated with the chain scissions are unzipping reactions, for example,

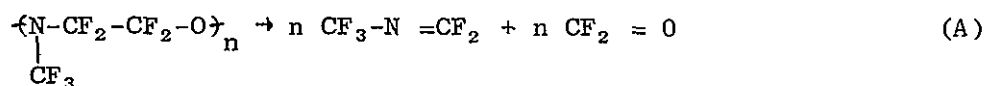


Table III

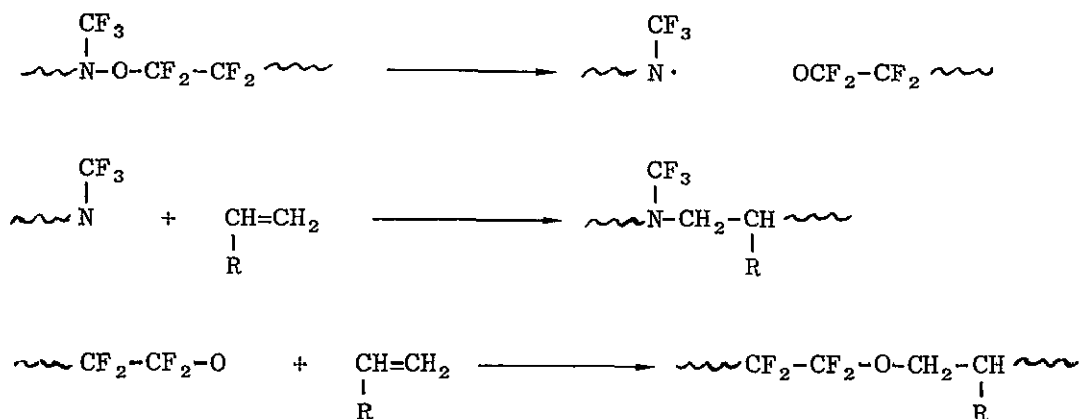
EMULSION POLYMERIZATION OF TRIFLUOROSTYRENE

Run No	Amount of Emulsifier, ^a g	Amount of Initiator, ^b g	Bis(4-amino-phenyl)disulfide	Reaction Time, hr	% Conversion to Product	Mol Wt	End-Group ^c Index
8610-83-7	IS 0 2	PPS 0 02	--	24	48	--	--
8610-83-8	DDA·HCL 0 2	PPS 0 02	--	24	70	--	--
8610-90-1	IS 0 2	AIBN 0 01	--	48	42	89,000	--
8610-90-2	IS 0 2	AIBN 0 01	0 01	48	38	(120,000) ^d	--
8610-90-3	IS 0 2	AIBN 0 01	0 03	48	42	55,000	--
8610-90-4	IS 0 2	AIBN 0 01	0 10	48	35	26,000	0 79
8610-94-1	IS 0 2	AIBN 0 012	0 03	45	40	--	0 91
8610-94-3	IS 0 2	AIBN 0 012	0 10	45	40	--	--
8610-100-1	DDA·HCl 0 2	AIBN 0 01	--	45	33	124,000	--
8610-100-2	DDA·HCl 0 2	AIBN 0 10	--	45	37	25,000	(0 26) ^e
8610-100-3	DDA·HCl 0 2	AIBN 0.01	0 03	45	48	--	0 49
8610-100-4	DDA·HCl 0 2	AIBN 0 01	0 10	45	34	23,000	0.95
8610-100-5	DDA·HCl 0 2	AIBN 0 01	0 30	45	34	(15,000) ^f	1 10
8610-105-1	DDA·HCl 0 3	AIBN 0 011	0 30	10	11	--	--
8610-105-2	DDA·HCl 0 3	AIBN 0 011	0 30	30	32	--	--
8610-105-3	DDA·HCl 0 3	AIBN 0 011	0 30	100	41	--	--
8610-105-4	DDA·HCl 0 3	AIBN 0 011	0 30	168 ^g	44	--	--

^aIS = Ivory Soap, DDA·HCl = dodecylamine hydrochloride, ^bPPS = potassium persulfate, AIBN = azobisisobutyronitrile

^csee experimental (Section IV-B), ^dprobably erroneous, ^eno band at 12.15 μ , ^fmol wt too low to be accurately determined by osmometry, ^gmore initiator added after 122 hours

The number of small fragments lost per chain scission depends on the experimental conditions. Thermal chain scission at 250°C is accompanied by the loss of about 1000 polymer repeat units, but scission by UV or γ radiation at 25°C is accompanied by the loss of only about 5 repeat units per scission⁷. Although a matter of considerable interest, the nature of the end groups in nitroso polymers is not yet established. Similarly, the stopping mechanism for the unzipping reaction, and for the end groups that are thereby incorporated into the polymer, is not yet established. It seems clear, however, that unzipping, like polymerization, is a radical (homolytic) process. Regardless of mechanism, the fact that limited unzipping accompanies chain scission suggests that chain scission generates polymeric radicals which should initiate the polymerization of monomers that are susceptible to free radical polymerization.



In this way block copolymers can be produced that will contain center segments derived from the nitroso elastomer and terminal segments of a second polymer.

2 Characterization of Nitroso Rubber

A large sample of nitroso rubber received from the Jet Propulsion Laboratory through the courtesy of D. D. Lawson was found to contain about 40% of an insoluble gel which was separated from the soluble material by Soxhlet extraction with Freon TF. Gel permeation chromatography (GPC) of

the soluble fraction indicated that it is a mixture of high-molecular-weight and very low-molecular-weight components. The mixture could be easily separated by a simple precipitation technique. Thus, 5.2 g of polymer was dissolved in 410 ml Freon TF, then 90 cc of acetone was added. The high-molecular-weight polymer precipitated (4.75 g) whereas the low-molecular-weight material remained in solution and was isolated by solvent evaporation (0.5 g). GPC measurements of each fraction showed that a clean separation had been obtained.

Vapor pressure osmometry in Freon TF of the low-molecular-weight component nitroso rubber indicates a molecular weight of 2600. Attempts to determine the molecular weight of the high-molecular-weight fraction by membrane osmometry in Freon TF at 37°C were not successful because of the low boiling point of the solvent.

A molecular weight of the high-molecular-weight fraction could, however, be obtained by membrane osmometry in perfluorotributylamine. A value of 760,000 was obtained, but, because of the high viscosity of the solution, this value may not be accurate. Light scattering in Freon-113 gave a molecular weight of 1,400,000. Intrinsic viscosity studies at 25°C in perfluorobutylamine,⁸ using $[\eta] = 8.77 \times 10^{-5} M_v^{0.66}$, gave a value of 1,400,000, in good agreement with the light-scattering value.

3 Cleavage Experiments

a Ultraviolet

Fractionated nitroso rubber was irradiated in quartz tubes for various lengths of time to correlate irradiation time with molecular weight. Initial work was carried out at 2537 Å using a Corning GS 754 Filter, but later work was carried out without a filter. No difference could be detected in the infrared spectra of the irradiated material when compared with the original material. The results are shown in Table IV. The minimum molecular weight attainable by continuous radiation appears to be around 200,000 to 250,000, reduced from the original 760,000. The values of \bar{M}_v do not decrease smoothly and continuously, but rather, erratic fluctuations are observed. The reason for the fluctuations is not clear.

Table IV

RESULTS OF IRRADIATION OF NITROSO RUBBER IN FREON TF

Notebook Reference	Grams FNR per 25 ml Freon TF	Irradiation Time (hours)	GPC Analysis Peak Count (% total area)	Intrinsic Viscosity* (dl/g)	Viscosity Average Molecular Weight, \bar{M}_v (g/mole)	Corning 754 Filter
8871-82-1	--	0 00	26 7(98%) 35 4(2%)	0 281	759,000	--
8871-86-1	0 4012	1 50	26 5(98%) 35 0(2%)	0 291	813,000	Yes
8871-87-1	0 4002	3 00	26 4(98%) 35 0(2%)	0 287	762,000	Yes
8871-89-1	0 4000	4 00	26 2(98%) 35 0(2%)	0 315	964,000	Yes
8871-91-1	0 4008	4 00	26 7(98%) 35 2(2%)	0 293	828,000	No
8871-92-1	0 4007	8 00	26 3(98%) 35 0(2%)	0 286	794,000	No
8871-95-1	0 4017	24 00	26 8(98%) 35 0(2%)	0 310	931,000	No
8871-98-1	0 4054	48 00	27 2(98%) 35 0(2%)	0 243	578,000	No
8871-96-1	0 4217	72 00	28 1(98%) 35 2(2%)	0 172	293,000	No
8871-100-1	0 4010	96 00	27 6(98%) 35 0(2%)	0 192	364,000	No
8871-102-1	0 4008	120 0	28 1(98%) 35 0(2%)	0 135	229,000	No
8871-106-1	0 4008	168 0	28 3(98%) 34 9(2%)	0 156	242,000	No
8871-109-1	0 4054	216 0	28 0(98%) 35 0(2%)	0 211	438,000	No

* Freon TF at 35 00°C

b. γ -Rays

To increase the number of cleavages per FNR polymer chain and thereby decrease the amount of AB block copolymer, a more intense radiation source is required. The gamma radiation from a Co-60 source would provide such intense radiation. Indeed, Shultz and coworkers⁷ have shown that a total gamma radiation dose of 6×10^6 rads reduces the \bar{M}_w of a nitroso rubber sample from $\bar{M}_w = 1,360,000$ to $\bar{M}_w = 125,000$. A study was

therefore carried out to determine the relationship of total gamma radiation dose to number of cleavages. The objective was to obtain FNR with $\bar{M}_v = 50,000 - 60,000$. The data are presented in Table V. As can be seen, a sufficiently large dose will produce the desired number of cleavages.

The infrared spectrum of 8871-140 was determined as a thin film cast from Freon TF. The spectrum contained all the peaks found in the spectrum of the starting FNR and only one additional one, a weak band at 5.61μ . This peak is probably caused by the presence of $CF_3-N=CF_2$ in the irradiated polymer. This species is a gaseous degradation product resulting from the gamma irradiation of nitroso rubber, pure $CF_3-N=CF$ absorbs at 5.55μ .

4 Copolymerization Experiments

Although a number of monomers could be considered as candidates for the outer high Tg segment, work was carried out only with chlorotrifluoroethylene. The following, general procedure was used. Fractionated nitroso rubber was dissolved in Freon TF, filtered through a coarse, sintered glass filter, and the solution evaporated into a quartz tube fitted with a ground glass joint and a thin neck for sealing under vacuum. The quartz tube was attached to a high-vacuum system, and chlorotrifluoroethylene distilled into the tube which was placed in a liquid nitrogen bath. The tube was sealed and the chlorotrifluoroethylene monomer allowed to swell the nitroso rubber for 30.0 hrs. The tube was then irradiated for the desired length of time and the polymer worked up as described in the next section. Results are shown in Table VI.

5 Characterization of Copolymer

a Fractionation

Since the irradiation of nitroso rubber in the presence of chlorotrifluoroethylene will produce a considerable amount of homopolymer, reaction mixtures are obtained that contain nitroso rubber homopolymer, polychlorotrifluoroethylene homopolymer, and block copolymers of various compositions. Thus, it is imperative to evolve a fractionation method for separating the block copolymer.

Table V
GAMMA IRRADIATION OF FRACTIONATED NITROSO RUBBER

FNR Sample	Dose Rate (Mrad/hr)	Dose Time (hr)	Total Dose (Mrads)	Intrinsic Viscosity* (dl/g)	Viscosity Average Molecular Weight, \bar{M}_v †	Cleavages per FNR Chain, N_c ‡	GPC Analysis GPC Count (% total area)
8871-132-1	0	0	0	0.250	611,000	0	26.2 (99%) 34.8 (1%)
8871-135	0.116	51.5	5.97	0.158	248,000	1.46	29.5 (99%) 34.8 (1%)
8871-138	0.116	78.1	9.06	0.143	205,000	1.98	30.2 (99%) 35.0 (1%)
8871-140	0.116	310.0	36.0	0.049	25,000	23.5	32.3 (98%) 36.0 (2%)

* The intrinsic viscosity was determined in Freon TF at $35.00 \pm 0.05^\circ\text{C}$

† The \bar{M}_v was obtained using the relationship $[\eta] = 2.80 \times 10^{-4} \bar{M}_v^{0.51}$

‡ The number of cleavages per chain is $N_c = \frac{M_1}{M_f} - 1$, where M_1 = initial molecular weight and M_f = final molecular weight

Table VI
BLOCK COPOLYMERIZATION EXPERIMENTS

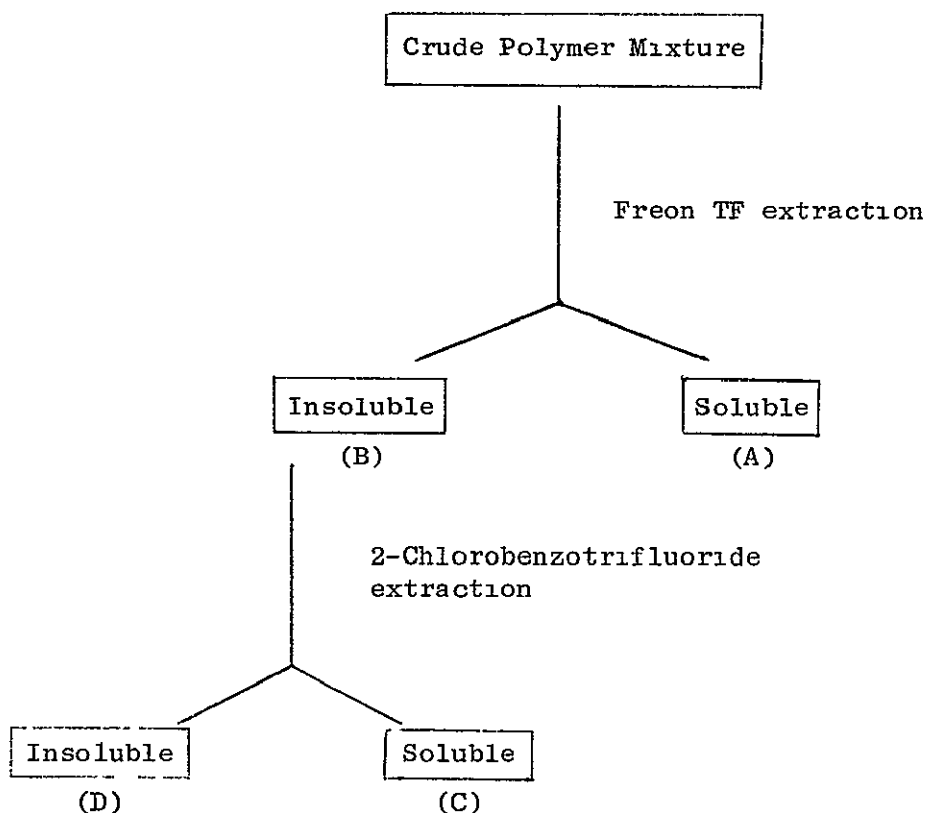
Experiment No	Feed Composition (g)		Percent Conv (g)	Irradiation Time	Fractionation (%)			No of * Cleavages
	Nitroso	CTE			Nitroso	PCTE	Block	
8871-113	3.45	6.00	85.5	40†	38.0	19.5	42.5	0.3
8871-127	2.99	0.50	90.5	40†	85.0	5.8	9.2	--
8871-136	3.52	6.00	94.8	51.5‡	33.8	11.7	61.3	3.5
8871-137	6.01	1.00	76.0	51.5‡	81.5	5.5	18.0	2.5
8871-146	2.90	3.00	91.2	64.6‡	52.0	4.8	43.2	23.5

* Calculated from $\frac{\bar{M}_v \text{ initial}}{\bar{M}_v \text{ final}} - 1$

† Ultraviolet

‡ Co-60

Considerable experimentation has shown that hot 2-chlorobenzotrifluoride dissolves polychlorotrifluoroethylene but not nitroso rubber and Freon TF dissolves nitroso rubber but not polychlorotrifluoroethylene. The following fractionation was thus carried out:



Fraction A is usually better than 95% nitroso rubber, and fraction C is usually better than 95% polychlorotrifluoroethylene. Fraction D is the desired block material.

b Mutual Solvent

To completely characterize the block materials, a solvent for them is essential. Because of the greatly different solubility characteristics of the two homopolymers, some time was expended in a search for a suitable solvent. Candidate solvents were screened according to the following experimental procedure:

To a small Pyrex extraction thimble was added approximately 0.4 g of Kel-F turnings and the thimble and contents dried in vacuo (65°C/6.0 hr). The thimble was next placed in a small Soxhlet extraction apparatus and the reservoir filled with 15 ml of test solvent. The extraction was carried out for a certain length of time after which the thimble was removed, washed with Freon TF, dried in vacuo (65°C 1.5 hr) and weighed. Those solvents capable of dissolving Kel-F at a reasonable rate were next tested for their ability to dissolve FNR. Results of these experiments are shown in Table VII. The most promising solvent found was chloropentafluorobenzene.

c Composition

The composition of the block copolymers was determined from their elemental analysis using percent nitrogen and percent chlorine. Even though pure nitroso rubber has a nitrogen content of only 7%, the accuracy of the analytical method was adequate.

An attempt was also made to determine the composition of the block copolymers by thermogravimetric analysis (TGA). Thus, it was found that at a heating rate of 10°C/min nitroso rubber degrades completely at 280-330°C, and polychlorotrifluoroethylene degrades at 395-450°C. In most cases, this method was found to yield composition values in reasonably good agreement with those obtained from elemental analysis.

Because of the clean degradation of nitroso rubber, polychlorotrifluoroethylene residues suitable for light-scattering studies might be obtainable. Such studies would give the molecular weight of the end segments. However, polymer obtained from TGA experiments was heavily charred and gave products unsuitable for light-scattering studies.

d Molecular Weight

An attempt was made to determine the molecular weight of the block copolymers by light-scattering experiments. However, light-scattering measurements were not possible using a 3% solution of 8871-113-1-2 in chloropentafluorobenzene at room temperature because of the extreme visual

Table VII
SCREENING OF POTENTIAL COMMON SOLVENTS FOR FNR AND KEL-F

Notebook Reference	Potential Solvent	Boiling Point (C°)	Extraction Time (hours)	Amount Extracted (grams)	Rate of Extraction (g/day)
8871-111-1	Perfluoro-2-butyltetrahydrofuran	99-107	96 0	0 0015	0 00038
8871-112-1	1,2-dichloro-hexafluoro-cyclobutane	59-60	46 0	0 000	0 000
8871-114-1	2,3-dichloro-octafluoro-butane	63	96 0	0 000	0 000
8871-105-1	Chloropenta-fluorobenzene	117	3.5	0 0292	0 200
8871-116-1	1,2-Dibromo-hexafluoro-propane	73	18 0	0 000	0 000

turbidity of the solution. This turbidity disappeared when the solution was heated to 110°C but reappeared when the solution was cooled to room temperature. Various cosolvents (Freon TF, perfluorotributylamine, 2-chlorobenzotrifluoride) were added to individual portions of the chloropentafluorobenzene solution in amounts ranging from 2 to 38% in the hope of clarifying the solution at room temperature. However, all the solutions remained highly turbid at room temperature, although they cleared upon heating. Light-scattering measurements could be carried out at 100-110°C to keep all the polymer in solution, but our light-scattering apparatus (Brice-Phoenix) is currently not set up for high temperature measurements, and lack of time precluded making the necessary modifications.

e Mechanical Properties

The block copolymers could be fabricated into sheets by either solution casting or compression molding. Solution-cast films 1.5 to 1.7 mils were prepared from 10% solutions of copolymer in chloropentafluorobenzene, and compression-molded films were prepared by heating at 300-350°F and 10,000 psi for about 15 sec.

Very poor mechanical properties were obtained. This, however, is not surprising considering the very low number of cleavages or the wrong percentage composition of the block copolymers, or both.

IV EXPERIMENTAL

A α,β,β -Trifluorostyrene

1. Anionic Polymerization

α,β,β -Trifluorostyrene was purchased from Pierce Chemical Company and purified by distillation (bp 46-49° at 29 torr). Anionic polymerizations were carried out in 200-ml argon-field beverage bottles using hypodermic syringes for reagent transfer. Gas liquid chromatographic analyses were carried out on a poly(methyl phenyl ether) column.

2 Free Radical Polymerization

Emulsion polymerizations were conducted in 30-ml serum bottles. Solid reagents were added to the argon-flushed bottles, the bottles were capped, and 1 ml of TFS was added with a syringe. After mixing thoroughly, 10 ml of deaerated water was added, the bottles were placed in a 55°C-water bath on a hot plate, and the contents were stirred magnetically. The polymers were isolated by adding the emulsions to methanol, filtering, redissolving the polymers in toluene or tetrahydrofuran, and again precipitating with methanol. Molecular weights were determined by osmometry. The relative amounts of aminophenylthio end groups were determined by comparing the infrared absorption at 11.90 μ (a band characteristic of PTFS) with the infrared absorption at 12.15 μ band to the 11.90 μ band. Thus the larger the index, the greater the concentration of end groups.

3. End-Group Reactions of Amino-Terminated PTFS

The amino-terminated PTFS was prepared by emulsion polymerization of TFS in the presence of bis(4-aminophenyl)disulfide. For the attempted coupling reactions, samples with a relatively high proportion of end groups were used (sample 8610-100-5 and similar samples). The samples had $M_n = 20,000$ or less, the functionality has not been determined.

Amino-PTFS (0.5 g) in 50 ml dry, purified THF was refluxed under nitrogen and treated first with 0.4 ml of an 0.01 g/ml solution of diphenylmethane diisocyanate in cyclohexane. Subsequently 0.5 ml more solution was added in 0.05 ml portions over a period of 5 days. The polymer (0.45 g) recovered after precipitation with methanol had a gel permeation chromatogram not significantly different from that of the untreated polymer. The infrared spectrum of the recovered polymer was unchanged in the 5.5 to 6.0 μ region. Then 0.2 g of the recovered polymer in 30 ml THF was refluxed for 12 hr with 10 ml of the 0.01 g/ml diisocyanate solution. The polymer recovered by precipitation with methanol now displayed weak absorption in the 5.5 to 6.0 μ region. Finally, the preceding recovered polymer (0.2 g) in 15 ml THF was refluxed for 4 hr with 0.2 g diisocyanate. The polymer recovered after precipitation with methanol had a noticeably enhanced, rather broad absorption in the 5.5 to 6.0 μ region. Elemental analysis for N was 0.35% (before treatment with diisocyanate, the N analysis was 0.34%, PTFS with no amino end groups gave an N analysis of 0.24%). In a comparison run aniline (0.2 ml, 2.2 mmole) and diisocyanate (0.3 g, 2.4 mg) in THF reacted quantitatively within a few minutes.

Amino-terminated PTFS (0.2 g) in 20 ml toluene was stirred at 25°C with 10% sodium hydroxide. During a 3 hr period the mixture was treated with a total of 0.7 ml (added in 0.025 to 0.2 ml portions) of a 0.01 g/ml solution of freshly sublimed terephthaloyl chloride in cyclohexane. The polymer recovered by precipitation with methanol gave a gpc trace nearly identical to that of the original polymer. The infrared spectrum also was not appreciably altered. Some of the recovered polymer (0.1 g) in 20 ml pyridine was mixed with 5 ml acetic anhydride. After 20 hr at 65°C the polymer recovered by precipitation with methanol showed a pronounced band at 5.8 μ . When 0.1 ml aniline and 0.2 g terephthaloyl in 10 ml toluene were stirred with 20 ml 10% NaOH at 25°C, the aniline reacted quantitatively within 5 min.

B. Nitroso Rubber

1 Fractionation

A large sample (ca 610 g) of crude nitroso rubber was received from Jet Propulsion Laboratory. This material was purified by extraction with Freon TF solvent in a large-scale Soxhlet extraction apparatus.

A portion of the crude nitroso rubber (348.6 g) was placed in the Soxhlet apparatus and extraction was started, after 256 hours, the polymer-rich Freon TF solution was removed and replaced with fresh solvent. Evaporation of the solvent from the polymer-rich solution gave 96.3 g (27.6%) of Freon TF-soluble polymer. A gel permeation chromatographic (GPC) analysis of this polymer showed peaks at GPC count 26.3 (high molecular weight material, ca 10-15%) and GPC count 34.8 (low molecular weight material, ca 85-90%).

The high molecular weight portion was recovered as follows: to a 3-liter beaker were added 26.0 g of Freon TF-soluble nitroso rubber (8871-79-1) and 1500 ml of Freon TF solvent. The solution was stirred and warmed (30°C) to dissolve the polymer. The solution was warmed to 35°C, kept at this temperature, and was vigorously stirred while reagent grade acetone (500 ml) was slowly added. After standing at room temperature for 3 days, the solution was decanted, and precipitated polymer was collected and dried in vacuo (67°C) to give 9.5 g (36.6%) of fractionated nitroso rubber (8871-79-2).

2 Irradiation

a Ultraviolet

To a 25-ml volumetric flask were added 0.4002 g of FNR and about 15 ml of Freon TF. The polymer was dissolved by shaking and heating the flask gently on a steam bath. The solution was diluted to the mark and quantitatively transferred to a quartz irradiation tube, and the tube sealed with a gas-oxygen torch. The quartz ampoule was irradiated for 3.0 hr with a Hanovia ultraviolet lamp and a Corning 754 filter that transmits uv radiation of 2537 Å. The quartz tube was opened, and the contents

were transferred quantitatively to a 25-ml volumetric flask. After dilution to the mark, 5 ml were removed and evaporated to provide for an intrinsic viscosity determination.

b X-Ray

The same procedure as in (a) was used except that a Co-60 source was used.

3 Copolymerization Experiments

Fractionated nitroso rubber (8871-82-1, 3.45 g) was dissolved in 100 ml of Freon TF and filtered through a coarse, sintered glass filter. The solution was evaporated into a quartz tube fitted with a ground glass joint and a thin neck for sealing under vacuum. The quartz tube was attached to a high vacuum system, and Kel-F monomer (6.00 g, 3.72 ml at -80°C) was distilled into the tube, which was placed in a liquid nitrogen bath. The tube was sealed and the Kel-F monomer allowed to swell the nitroso rubber for 30.0 hr. The tube was then irradiated for the desired length of time and the crude polymer recovered.

REFERENCES

- 1 D Livingston, P Kamath, and R Corley, J Polym. Sci., 20, 485 (1956).
- 2 F D. Trischler and J Hollander, Polymer Previews, 3, 229 (1967)
3. D. D Smith, R. M Muich, and D. R. Pierce, Ind Eng. Chem., 49, 1241 (1957)
- 4 M Szwarc, Fortschr Hochpolymer Forsch , 2, 275 (1960).
- 5 A. J. Constanza, Macromol Synthesis, 2, 87 (1966)
- 6 M. Prober, J. Am Chem. Soc., 75, 968 (1953)
- 7 A R Shultz, N. Knoll, and G A Morneau, J Polym Sci ; 62, 211 (1962)
- 8 G A Morneau, P I Roth, and A. R Shultz, J. Polym Sci , 55, 609 (1961)

APPENDIX

A Dynamic Approach to Diffusion and Permeation Measurements

by

R.A. Pasternak, J.F. Schimscheimer,
and J. Heller

Polymer Chemistry Department
Stanford Research Institute
Menlo Park, California

INTRODUCTION

The measurement of diffusion, permeation, and solubility is of considerable practical and theoretical interest. Diffusion and solubility coefficients are usually determined by observing the weight change of a polymer sample during sorption, while diffusion and permeation coefficients are obtained by following the flow of a permeant through a membrane.

In the standard approach to permeation studies, developed by Barrer and coworkers¹ and others,² a pressure differential is established across a membrane, and the pressure in the downstream volume is measured as a function of time. After a gradual rise, the pressure increases linearly with time when steady-state permeation is established. The slope of the linear portion is proportional to the permeability coefficient, and its intersection with the time axis, the so-called time lag, is inversely proportional to the diffusion coefficient. This closed-volume method has several weaknesses, in particular, the pressure differential requires mechanical support for the membrane and vacuum-tight seals. However, the most serious limitation, which also applies to sorption methods, is a basic one, the entire amount of vapor permeated, or sorbed, from the beginning of the experiment is accumulated and measured as a function of time. The measuring precision is usually not sufficient for a detailed analysis of the data in terms of transient permeation rates and of slow drifts caused by time-dependent changes in membrane properties.

This paper presents a dynamic approach to the measurement of permeation and diffusion coefficients, which is largely free of these drawbacks.

A flow system, in which both sides of the membrane are at atmospheric pressure, is employed, and permeation rates through the membrane are measured continuously.

After completion of this work, a study came to our attention in which the same basic concept was employed for measuring the steady state permeation of gases through polymer films.³

Mathematical Treatment

The permeation flux, F , through a membrane of thickness ℓ is given by

$$F(x) = -D \frac{dc}{dx} \quad (1)$$

where c is the concentration of the permeant in the membrane at a position x . In our treatment, it is assumed that the diffusion coefficient D is not a function of the concentration, that the concentration is proportional to the pressure of the permeant, and that swelling of the membrane is negligible. We are interested only in the flux at $x = \ell$.

The following generalized boundary conditions are characteristic for permeation studies

$$\begin{array}{lll} c = 0 & x = \ell & t \geq 0 \\ c = c_1 & x = 0 & t = 0 \\ c = c_f & x = 0 & t > 0 \\ c = c_1 (\ell - x)/\ell & 0 \leq x \leq \ell & t = 0 \\ c = c_f (\ell - x)/\ell & 0 \leq x \leq \ell & t = \infty \end{array}$$

These boundary conditions represent the change from one steady state to another, with the pressure of permeant on the downstream side of the membrane always kept at zero, either c_1 or c_f , the initial and final concentrations at $x = 0$, can of course be zero. Two useful solutions of the differential equation (1), which were obtained by generalizing expressions given in the literature,^{4,5} are

$$F = \frac{Dc_1}{\ell} + \frac{D(c_f - c_1)}{\ell} \left[1 + 2 \sum_{n=1}^{\infty} (-1)^n \exp \left(- \frac{n^2 \pi^2 D t}{\ell^2} \right) \right] \quad (2)$$

$$F = \frac{Dc_1}{l} + \frac{D(c_f - c_1)}{l} \frac{4}{\sqrt{\pi}} \sqrt{\frac{l^2}{4Dt}} \sum_{n=1,3,5,\dots}^{\infty} \exp\left(-\frac{n^2 l^2}{4Dt}\right) \quad (3)$$

where Dc_1/l and Dc_f/l are the steady-state fluxes at time $t = 0$ and $t = \infty$, respectively. $\Delta F = F - Dc_1/l$ represents the change in flux during the experiment; it has at steady state a limiting value of $\Delta F_{\infty} = D(c_f - c_1)/l$.

The series of Eqs. (2) and (3) converge at large and small values of t , respectively. It is reasonable to retain only the first term when the second term contributes less than 2% to the sum. It can be shown that for eq. (2) this condition is satisfied for $\Delta F/\Delta F_{\infty} > 0.46$. Equation (2) can then be rewritten as

$$(\Delta F_{\infty} - \Delta F) = 2\Delta F_{\infty} \exp(-\pi^2 Dt/l^2) \quad (2a)$$

A plot of $\log (\Delta F_{\infty} - \Delta F)$ versus t is a straight line with a slope which is proportional to the diffusion coefficient. Such a plot would be quite sensitive to the choice of ΔF_{∞} , which in real systems may not be truly constant but may increase slowly with time.

The first-order approximation of eq. (3)

$$\Delta F = \Delta F_{\infty} \frac{4}{\sqrt{\pi}} \sqrt{\frac{l^2}{4Dt}} \exp\left(-\frac{l^2}{4Dt}\right) \quad (3a)$$

holds over a very wide range, namely for $\Delta F/\Delta F_{\infty} < 0.97$. A plot of $\log (\Delta F \sqrt{t})$ versus $1/t$ is a straight line with a slope inversely proportional to D .⁵ This method of evaluating the data requires a precise definition of $t = 0$ and is computationally rather inconvenient.

A more convenient relationship evolves by rewriting Eq (3a) as

$$\Delta F/\Delta F_{\infty} = (4/\sqrt{\pi})X \cdot \exp(-X^2) \quad (3b)$$

where $X^2 = l^2/4Dt$. The right side of Eq. (3b) is the second derivative of the error function. A plot of $\Delta F/\Delta F_{\infty}$ versus $1/X^2$, constructed from values given in the literature,⁴ is shown in Fig. 1. It represents a normalized permeation rate curve with ΔF expressed as the fraction of the steady-state flux ΔF_{∞} and t expressed in units of $4D/l^2$. By comparing

any experimental curve with this theoretical curve, the diffusion law can be verified and the diffusion coefficient derived. Values of $1/X^2$ for simple fractions of $\Delta F/\Delta F_\infty$ are taken from Table I (a numerical representation of Fig. 1), and the times t are read off the experimental curve for the corresponding values of $\Delta F/\Delta F_\infty$. If D is a constant, the plot of $1/X^2$ versus t is a straight line with a slope of

$$d(1/X^2)/dt = 4D/\ell^2 \quad (4)$$

A simplified method can be used also, it depends on the fact that the curve in Fig. 1 has a rather extended linear range with an empirical slope of $d(\Delta F/\Delta F_\infty)/d(1/X^2) = 1.42$. When the definition of X given in Eq. (3b) is introduced, one obtains

$$D = 0.176\ell^2 (d\Delta F/dt) \quad 1/\Delta F_\infty \quad (5)$$

where $d\Delta F/dt$ is the slope of the linear part of the experimental curve. The uncertainty in ΔF_∞ contributes only linearly to that of D .

In the actual experiment (see next section), a carrier gas sweeps at a constant flow rate f through the permeation cell and the detector. The increase in the detector signal ΔS with respect to that at $t = 0$ is proportional to the concentration increment, Δm , of the permeant in the carrier gas. This concentration increase is related to the change in permeation flux, ΔF , by the condition of mass balance

$$A \quad \Delta F = f\Delta m + V(dm/dt) = fk\Delta S + Vk(dS/dt) \quad (6)$$

where A is the membrane area, V is the cell volume, and k is the sensitivity of the detector for a particular permeant. For desorption, ΔF , Δm , and ΔS are negative.

The volume term, which expresses concentration changes within the cell and is of course zero at steady state, decreases with increasing f/V ratios (in the present instrument it is about unity) and with decreasing rate of change in signal dS/dt . $1/\Delta S$. This term can be minimized by appropriate choice of f/V and is in any case only significant for a transient state of short duration.

TABLE I
 NUMERICAL VALUES FOR NORMALIZED, THEORETICAL
 PERMEATION CURVE (see Fig 1)
 Relative flux $\Delta F/\Delta F_{\infty}$ versus normalized time $1/X^2 = (4D/\ell^2)t$

$\frac{\Delta F}{\Delta F_{\infty}}$	$\frac{1}{X^2}$	$\frac{\Delta F}{\Delta F_{\infty}}$	$\frac{1}{X^2}$
0 05	0 220	0 55	0 600
0 10	0 265	0 60	0 650
0 15	0 300	0 65	0 705
0 20	0 335	0 70	0 770
0 25	0 370	0 75	0 845
0 30	0 405	0 80	0 940
0 35	0 440	0 85	1 045
0 40	0 475	0 90	1 210
0 45	0 510	0 95	1 570
0 50	0 555		

Apparatus and Procedure

A schematic drawing of the apparatus is shown in Fig. 2 and is self-explanatory. The permeation cell C and gas lines to the cell, coiled 1/16-inch metal tubes, were in a thermostated air bath, whereas flow controller Fc, the flow meter Fm, and detector D were kept at ambient temperature, approximately 25°C. The membrane M was clamped between two flat surfaces of the glass permeation cell, and a trace of silicon grease was used as sealant. The exposed circular area of the membrane was 2.8 cm², and the volume of each cell compartment was less than 1 cm³. A thermal conductivity detector was used.

In the operational procedure, the system is purged by passing a rapid stream of helium through both compartments of the cell. Constant flow is then established through the downstream compartment and the detector is zeroed. If the membrane is mounted airtight, diversion of the helium stream through the bypass does not produce a change in signal. Pinholes in the membrane can be detected by introducing a gas of low permeation rate, e.g., nitrogen, into the upstream compartment and watching for the appearance of a significant signal.

In an actual run, the upper compartment is again filled with helium to reestablish the detector zero. The permeant is then introduced into the cell by throwing the valves, it may be a gas, a vapor, a helium-permeant mixture of known composition, or a liquid.* As the permeant diffuses through the membrane, it is carried by the helium stream to the detector, and the resulting signal is continuously recorded. The concentration of the permeant on the downstream side of the membrane is held at an insignificant level by selecting a flowrate appropriate for the particular permeation rate under study.

An alternative mode of operation can be employed for very low permeation rates. The permeant is collected in the closed-off cell for a given time interval, and meantime the helium is diverted through the bypass. The helium stream is then switched back through the cell, and the peak is recorded. Its area is a measure of the amount permeated through the membrane during the time interval.

*For studies of liquids, a modified cell with a rubber septum for injecting the liquid into the upstream compartment is used.

Calibration

Thermal conductivity cells of standard design show linear response to the partial pressure of the contaminant in the carrier gas, at least at low concentrations. Since the reliability of the method described here depends primarily on the performance of the detector and in particular on its linearity, a number of calibrations were carried out.

(1) A gas mixture containing 0.21 vol. % carbon dioxide in helium produced a signal which was independent of flow rates between 0.5 and 2 cm³/sec and at temperatures between 30 and 52°C. The zero balance changed markedly with flow rate, but only slightly with temperature. The sensitivity of the detector-recorder combination was 2.0 ppm CO₂/mm deflection, for the detector current of 200 mA employed throughout this study. At standard conditions of one atmosphere and 25°C, this equals 3.80×10^{-9} g CO₂/cm³ mm. Even at maximum sensitivity the zero drifts during permeation runs were well below 1 mm, this indicated very stable flow rate and heating current.

(2) At steady-state permeation of CO₂, O₂, and N₂ through a polyethylene membrane, the signal was measured as a function of flow rate of the carrier gas. Data for a typical run with O₂ are given in Table II. The product of flow rates and signal was constant within the precision of the measurements, as expected for a detector with linear response.

(3) The permeant was collected for a defined time interval in the closed-off downstream compartment and the helium stream was then switched back to the cell. The results of one experimental series are shown in Table III. The peak areas, which are here approximated by the product of height and halfwidth (compare with the planimeter values given in parenthesis), were found to be proportional to the collection time within the precision of the measurements. The average area per second, 1.33 cm², was about 10% lower than the equivalent area at steady state, this difference may be due to absorption effects.

(4) Steady-state permeation of liquid hexane through a polyethylene membrane was established, the resulting signal measured, and its absolute

TABLE II
CORRELATION BETWEEN FLOW RATE AND SIGNAL
AT CONSTANT PERMEATION RATE OF OXYGEN THROUGH
A POLYETHYLENE MEMBRANE AT 30°C

FLOW RATE*	2 0	2 3	2 5	3 0	4 0	5 0	6 5	8 0	10 0
SIGNAL	89	80	75	65	50	39 5	29	24	18
PRODUCT	178	184	188	195	200	197	189	192	180

* ARBITRARY UNITS, 4 6 = 1 0 ml/sec

TABLE III
CORRELATION BETWEEN PEAK AREA AND ACCUMULATION TIME AT CONSTANT
PERMEATION RATE OF OXYGEN

TIME (sec)	PEAK		PEAK AREA (cm ²)	AREA/sec (cm ² /sec)
	HEIGHT (cm)	HALF WIDTH (cm)		
STEADY STATE	6 8	21 2*	144	1 44
50	37 6	1 80	68	1 36
100	72 8	1 85	135	1 35 (1 36)
150	102 0	1 85	200	1 33
200	131 0	2 00	262	1 31
300	180 0	2 17	382	1 27 (1 32)

*FOR 100 sec

rate was determined by condensing the hexane vapor carried by the helium stream. Although the signals at 30 and 52°C differed by a factor of three, the sensitivities at the two temperatures, 3.41 and 3.48×10^{-9} g/cm³ mm, were identical within the precision of the measurements.

The ratio of the detector sensitivity for carbon dioxide and hexane, 1.1, agreed, within the combined limits of errors, with the ratio of 1.3 derived from the literature.⁶ Thus it appears justified to use as first approximation the literature values⁶ for the relative sensitivities of different gases and vapors.

Finally, the dependence of the permeation rates on the gas flow through the upstream compartment was explored. No effects were found at steady state. The transient state was, however, sensitive to flow rate. A flow-dependent delay in the appearance of the signal can be ascribed to the time required for the permeant to flow from the valves to the membrane and from the downstream compartment to the detector. (In the present experiments, this delay was about 30 sec.) In addition, the slope of the transient signal increased with increasing flow rate to approach a constant value. Apparently, at lower flow rates the first gas is only gradually replaced by the second, whereas at high flow rates a reasonably sharp boundary moves through the cell. Since the boundary cannot be infinitely sharp, the observed slope and the diffusion coefficient derived from it are in principle always smaller than the theoretical ones. This error will be significant only for a very fast approach to steady state, as was observed for the thin membranes, and can be minimized by appropriate design of the cell and by reduction of the replaced gas volume.

Permeation and Diffusion Data

The permeability coefficients of CO₂, O₂, N₂, and liquid hexane through low-density polyethylene membranes of commercial origin were measured at temperatures between 25 and 52°C. Diffusion coefficients were determined for CO₂ at a series of temperatures, for O₂ and N₂, either the signals were too small or steady state was reached too fast to permit reliable measurements of the transient state.

A typical CO₂ permeation curve for a 3.4-mil film is shown in Fig. 3a. The transients for absorption and desorption are identical within the precision of the measurements. (The zero signal represents the baseline for absorption and the steady-state signal represents the baseline for desorption.) The identity of the absorption and desorption curves is in agreement with the diffusion rate law expressed by Eqs (2) and (3). Figure 3b is a plot of $1/X^2$ versus t for the absorption step. (See section on Mathematical Treatment.) A straight line is obtained over almost the entire range. A diffusion coefficient $D = 3.9 \times 10^{-7}$ cm²/sec was derived from its slope by means of Eq. (4), it agrees closely with the value $D = 3.8 \times 10^{-7}$ cm²/sec derived by the approximation, Eq (5)

In Fig. 4, the logarithm of the steady-state signals S_{∞} for permeation of CO₂, O₂, and N₂ is plotted versus the reciprocal absolute temperature. Straight lines are obtained from which the heats of permeation are derived. The signals S_{∞} are converted to absolute permeation rates by multiplying them by the product of flow rate f and the calibration constant k for CO₂. The O₂ and N₂ values are further multiplied by correction factors which take into account the relative sensitivity of the detector for the gases. These factors, 1.20 for O₂, and 1.09 for N₂, are calculated from data given in the literature.⁶

Table IV summarizes permeation and diffusion coefficients at 25°C and heats of permeation and diffusion for the different membranes studies. The overall consistency of the data and the agreement with the literature data,⁷ which are also shown, is quite satisfactory. The low value of the heat of diffusion for CO₂, particularly for the thinner membrane, is probably an artifact due to the finite time required to replace the helium by CO₂ in the upstream compartment (see above).

Finally, the applicability of the method to liquid permeants is illustrated with some data obtained for n-hexane and a 3.5-mil membrane. A permeation run at 25°C is shown in Fig. 5a. The plot of $1/X^2$ versus t , Fig. 5b, is again linear over a wide range, however, it is displaced along the time axis and also may have a significant curvature at larger

Table IV

DIFFUSION AND PERMEATION DATA (temperature range 25-52°C)

	l (mil)	$P_{25} \times 10^{10}$ $\left(\frac{\text{cc (St}_p\text{)}/\text{cm}}{\text{cm}^2 \text{ sec cm Hg}} \right)$	E_p $\left(\frac{\text{kcal}}{\text{mole}} \right)$	$D_{25} \times 10^7$ $\left(\frac{\text{cm}^2}{\text{sec}} \right)$	E_D $\left(\frac{\text{kcal}}{\text{mole}} \right)$
CO ₂	1.2	12.9	8.2	-	-
	3.4	11.6	9.0	-	-
	3.4	10.9	10.0	3.0	7.5
	5.0	10.6	10.4	3.7	8.1
	*	12.6	9.3	3.72	9.2
O ₂	1.2	3.4	9.2		
	3.4	2.2	11.7		
	*	2.9	10.2		
N ₂	1.2	0.84	10.6		
	*	0.98	11.8		

*Ref. 7

values of S/S_∞ . These deviations from simple theory, which were also found for benzene as permeant, require further study; they may be due to concentration dependence of the diffusion coefficient.⁸

The steady-state permeation rates for hexane (or benzene), though time independent, were very sensitive to the temperature history of the membrane. After exposing the membrane to hexane at a higher temperature, the permeation rate at a specific lower temperature increased significantly, the more so the higher the upper temperature. For example, the rate at 25° tripled after heating to 52°C, but within this temperature range the permeation rates now became reproducible. The data are shown in Fig. 6 in the form of a (linear) Arrhenius plot. The heat of permeation was found to be 9.3 kcal/mole. The Arrhenius plot constructed from literature data⁹ indicates a value of 17 kcal, we suspect that in these measurements the irreversible and reversible temperature effects were not separated.

Further Elaboration of the Method

The effectiveness of the method for the measurement of diffusion and permeation rates has been illustrated with a few examples. The sensitivity of the prototype instrument, which is sufficient for many applications, can be augmented a thousandfold or more by reducing the flow rate, increasing the membrane area, and introducing a more sophisticated detector.* Moreover, the addition of a gas chromatographic column would permit the study of permeating mixtures.³

The dynamic approach provides also a powerful tool for the study of transitions in polymers. Since transitions are usually associated with a significant change in permeability, slow temperature scanning under quasi-steady-state conditions should result in permeation rate curves with discontinuities at the transition points. Such a temperature-permeation curve is shown in Fig. 6 for the system CO₂-vulcanized

*A refined version of the instrument is being built by Dohrmann Instruments Co. (a subsidiary of Infotronics), Mountain View, California, under license from Stanford Research Institute.

gutta-percha The rapid increase in the rate at about 43°C coincides with the known melting point of the polymer and has been reported previously.¹⁰

Diverse other applications of the instrument are suggested. For example, binary gas mixtures of well-defined composition can be prepared by appropriate choice of membrane temperature and flow rate of the carrier gas.

Acknowledgment

This research was supported in part by the Jet Propulsion Laboratory, California Institute of Technology, sponsored by the National Aeronautics and Space Administration under Contract NAS 7-523, and in part by Stanford Research Institute. The authors are greatly indebted to Mr. Leonard McCulley for guidance in respect to the mathematical treatment presented here.

REFERENCES

1. R. M. Barrer and G. Skirrow, J. Polymer Sci., 3, 549, 564 (1948).
2. Reviews in Diffusion in Polymers, J. Crank and G. S. Park, Eds., Academic Press, New York, 1968.
3. T. L. Caskey, Modern Plastics, 45, 447 (1967).
4. J. Crank, The Mathematics of Diffusion, Clarendon Press, Oxford, 1956, p. 47.
5. W. A. Rogers, R. S. Buritz, and D. Alpert, J. Appl. Phys., 25, 868 (1954).
6. R. Kaiser, Gas Chromatography, Butterworths, Washington, D. C., 1963, pp. 92-94.
7. A. S. Michaels and H. J. Bixler, J. Polymer Sci., 50, 413 (1961).
8. R. M. Barrer and R. R. Fergusson, Trans. Faraday Soc., 54, 989 (1958).
9. M. Salame, SPE Trans., 1, 153 (1961).
10. G. J. van Amerongen, J. Polymer Sci., 2, 381 (1947).

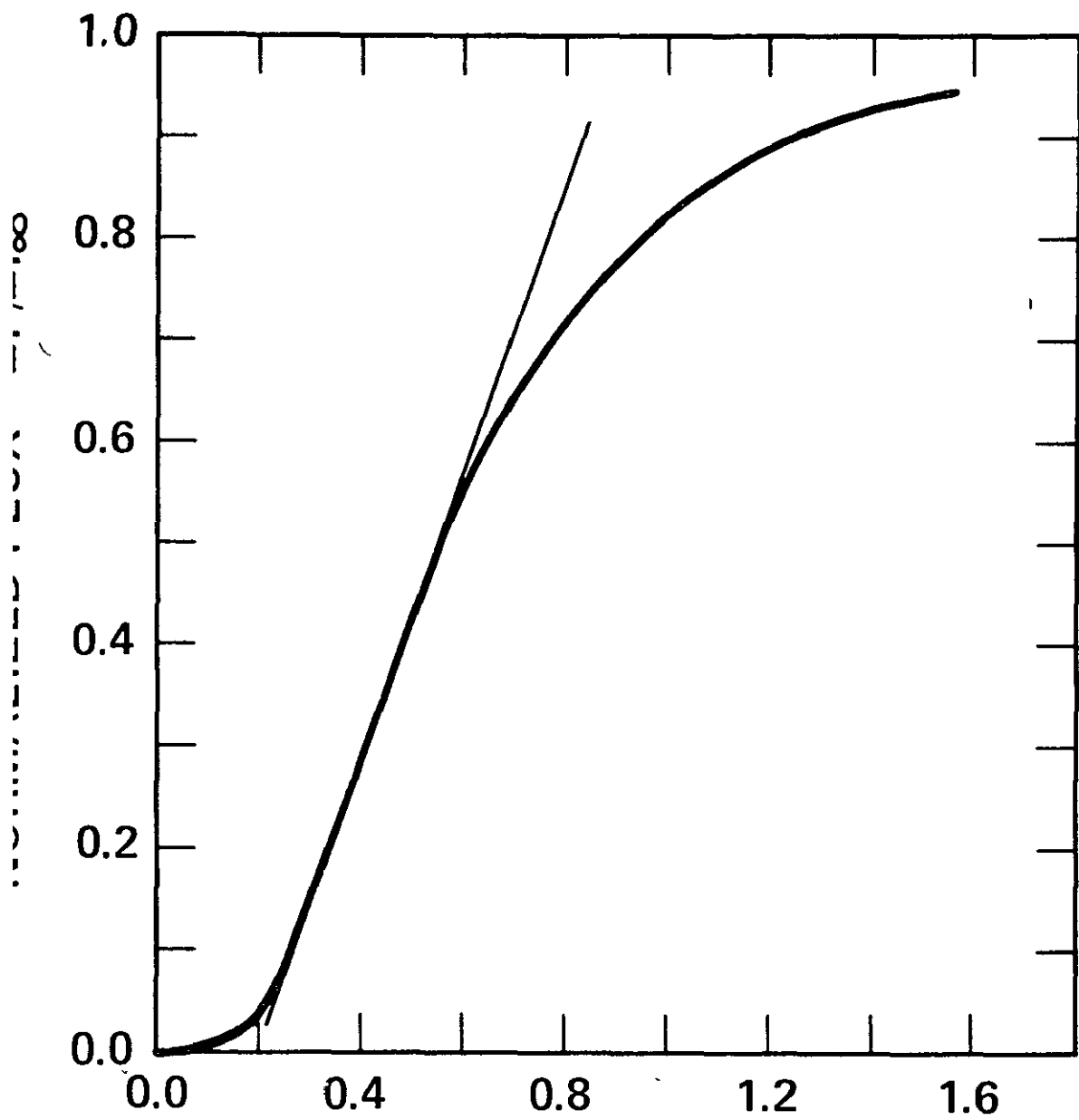
PRECEDING PAGE NOT FILMED

ILLUSTRATIONS

- Fig. 1 Theoretical permeation curve for constant diffusion coefficient.
- Fig. 2 Schematic drawing of the unit G, carrier gas; Fc, flow controller, Fm, flow meter, C, permeation cell, u, upstream compartment, d, downstream compartment, B, bypass, M, membrane, D, detector, R, recorder; T, valves to carrier gas, permeant gas, or vapor source reservoirs, V, three-way valves.
- Fig. 3 (a) Experimental curve for permeation of CO_2 through a 3.4-mil polyethylene membrane (at 30°C and flow rate of 0.5 cc/sec). CO_2 was introduced at A, He at B. (b) Plot of $1/X^2$ versus time t .
- Fig. 4 Steady-state permeation of CO_2 , O_2 , and N_2 through a 1.2-mil polyethylene membrane, plots of logarithm of the steady-state permeation signal S_∞ versus the reciprocal temperature $1/T$.
- Fig. 5 (a) Experimental curve for permeation of hexane through a 3.5-mil polyethylene membrane (at 25°C and flow rate of 1 cc/sec). At A, liquid hexane was introduced into the cell. (b) Plot $1/X^2$ versus time t .
- Fig. 6. Arrhenius plot for steady-state permeation of hexane through a 3.5-mil polyethylene membrane, the transmission rate Q is expressed in units of g mil/m² 24 hr.
- Fig. 7 Steady-state permeation rate of CO_2 through a 3-mil vulcanized gutta-percha membrane. Temperature scanning rate about $0.5^\circ\text{C}/\text{min}$. Permeation rate is given in arbitrary units.

PRECEDING ILL.

NOT FILMED



$$1/X^2 = (4D/l^2) \cdot t$$

TA-364,522-141

FIG 1

LOADING PAGE PLANK NOT FILMED

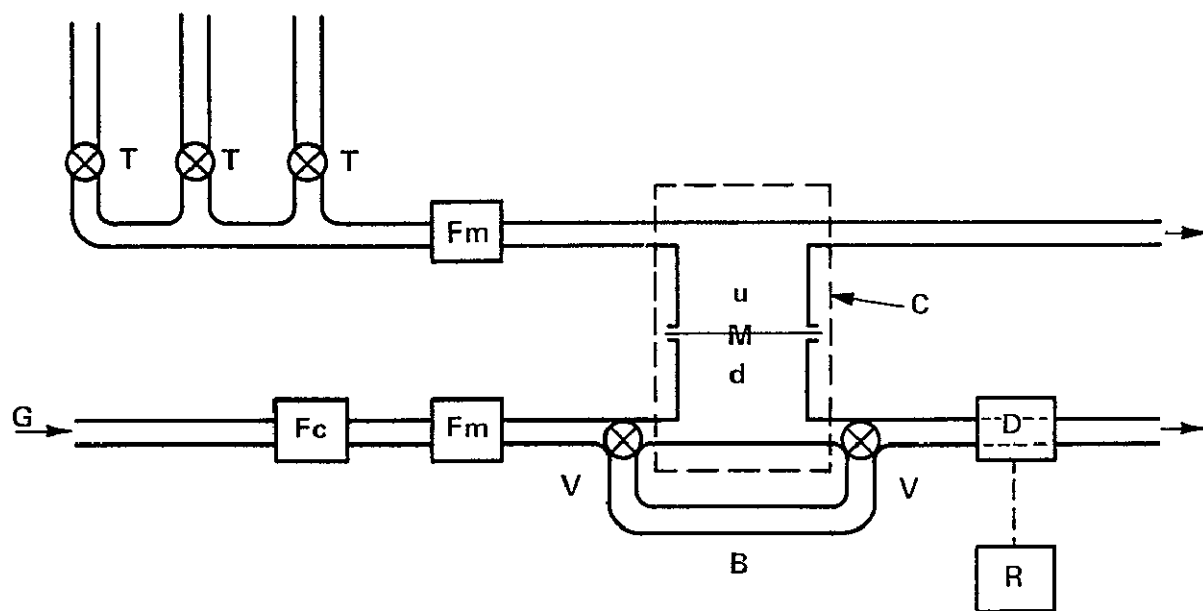
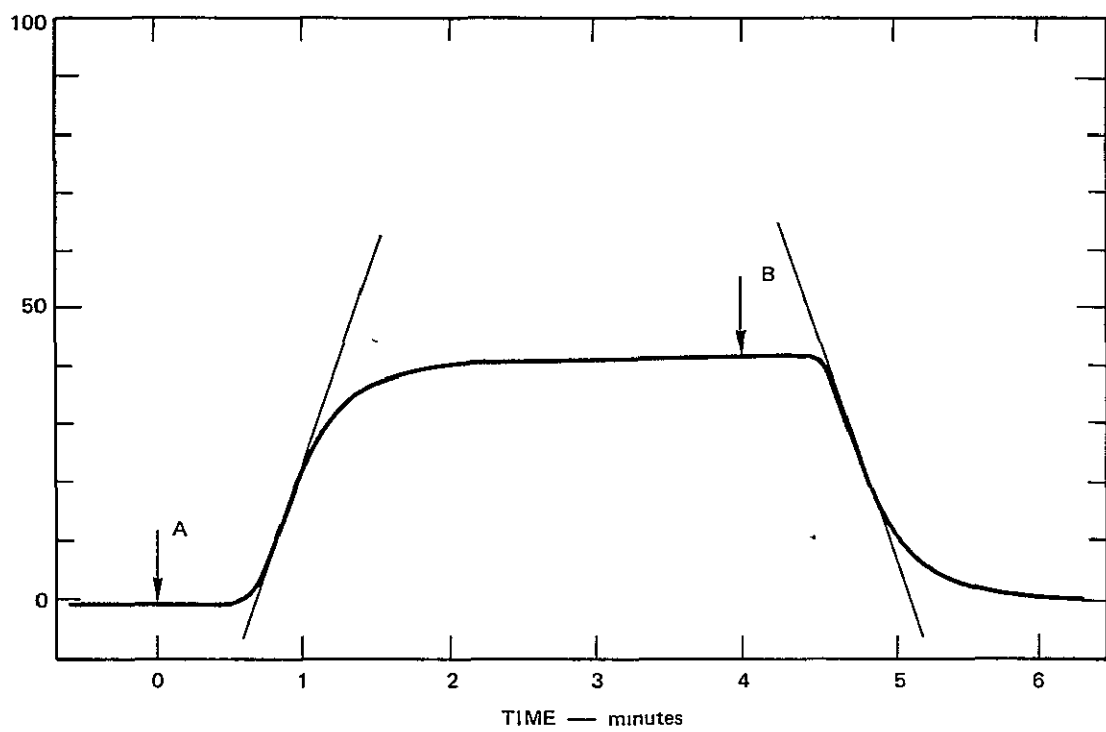


FIG 2



TA-321581-1

Figure 3A

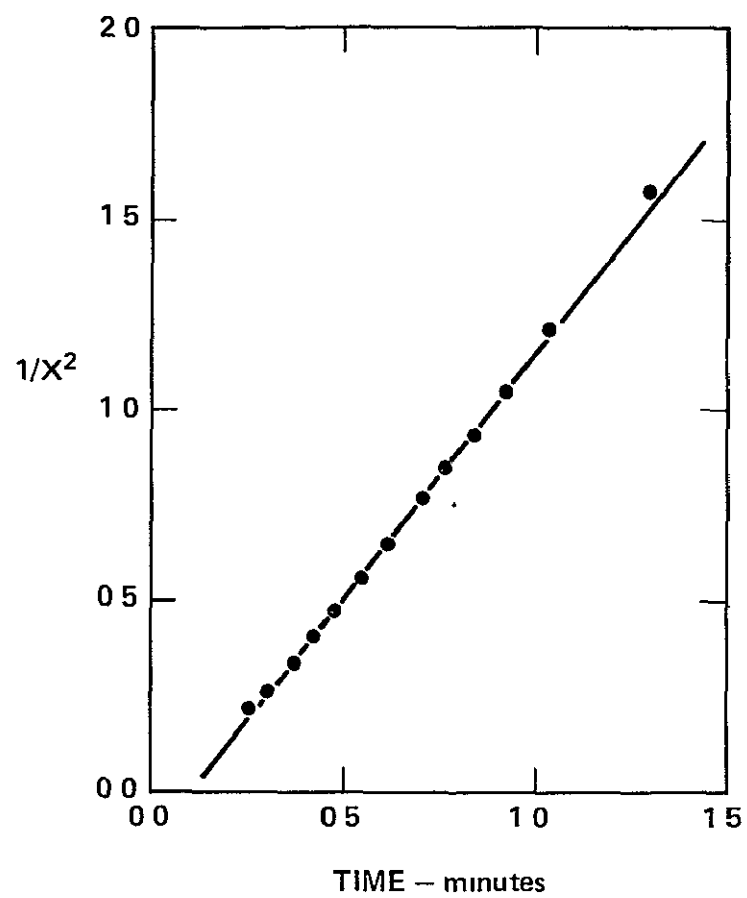


FIG 3B

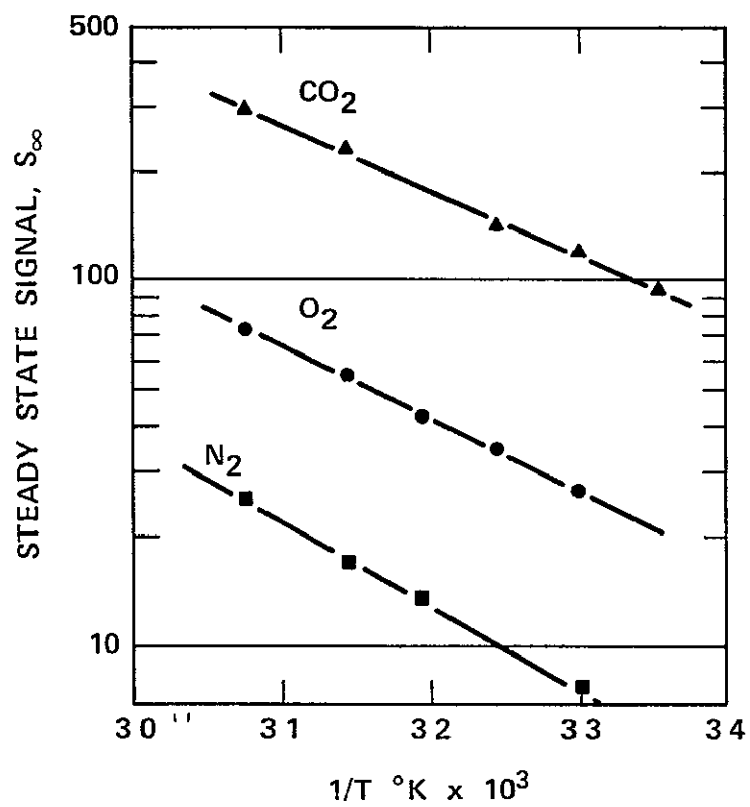


FIG 4

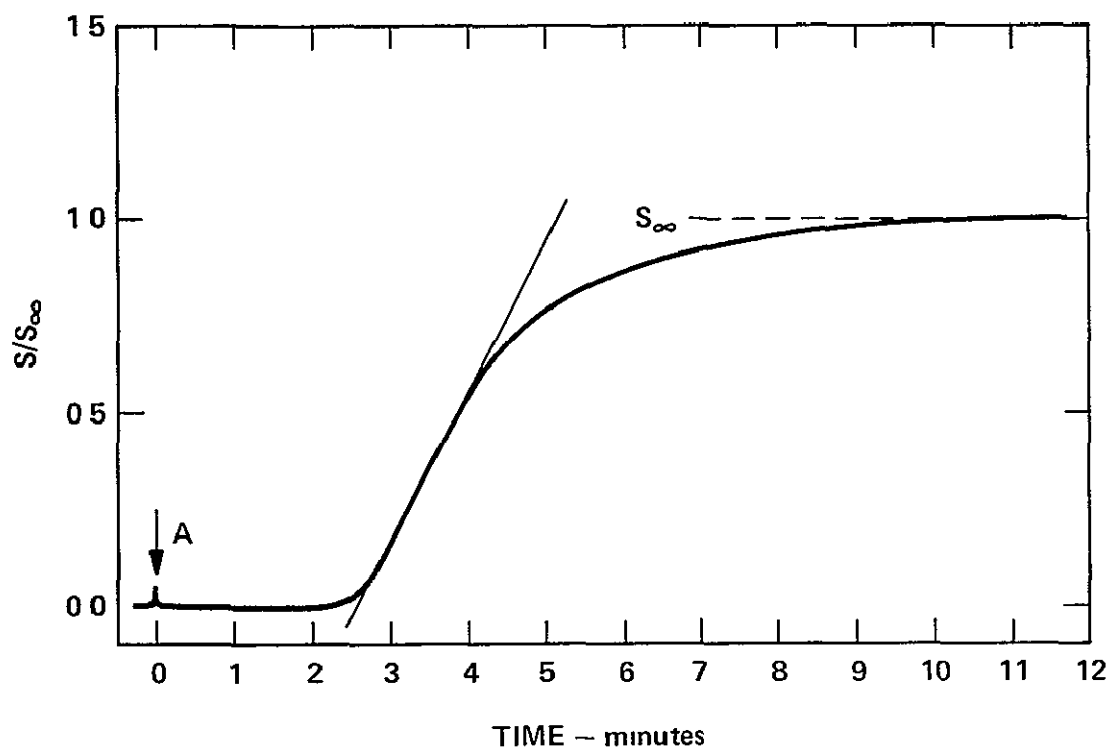
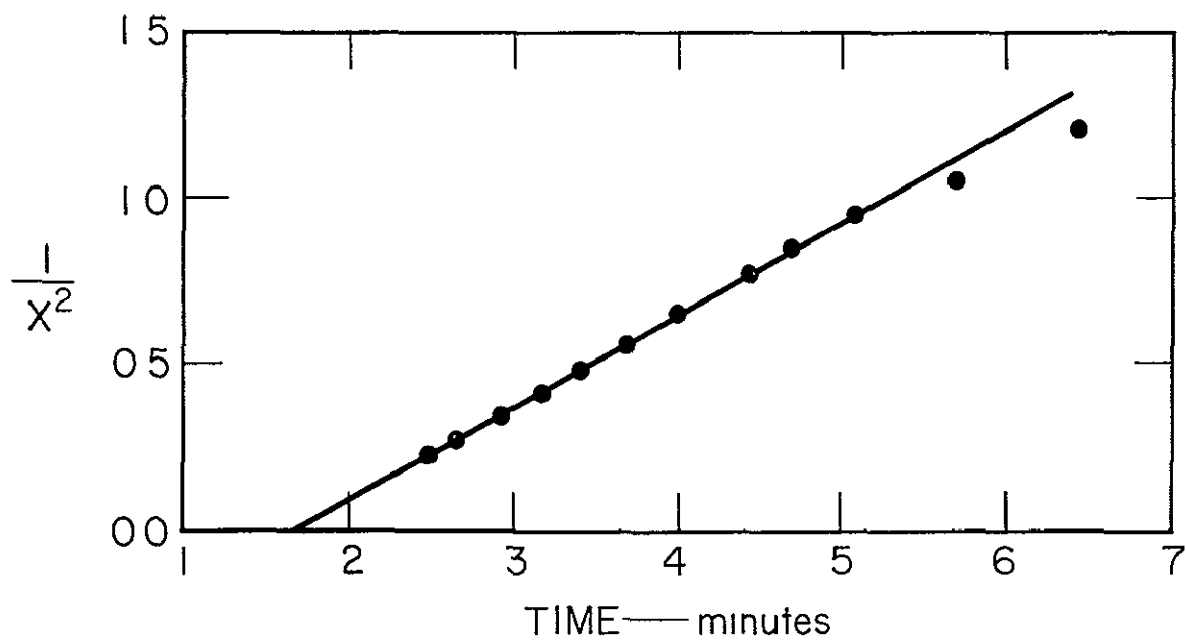


FIG 5A



TB-364,522-142

FIG 5B

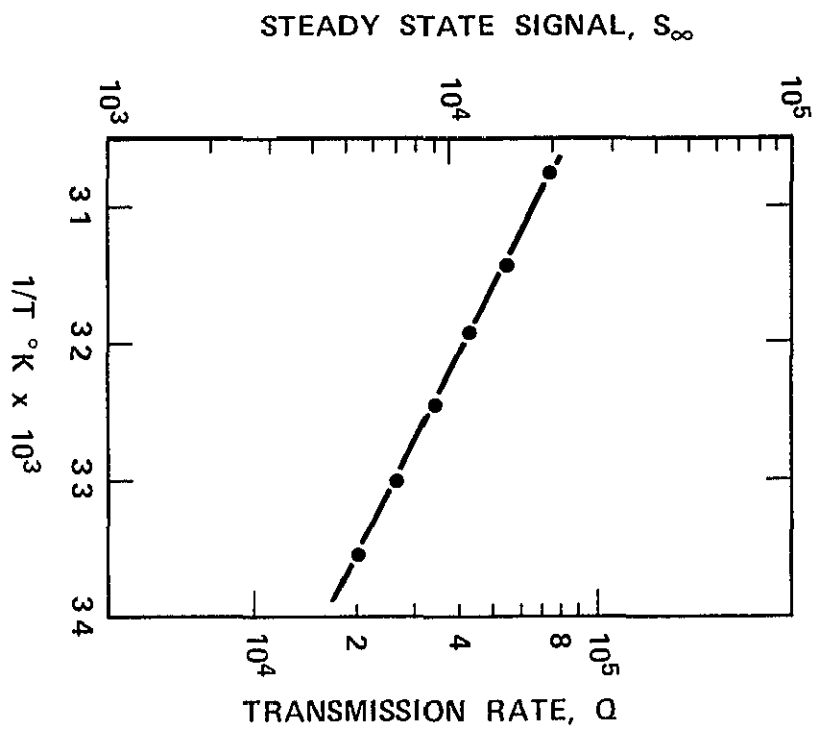
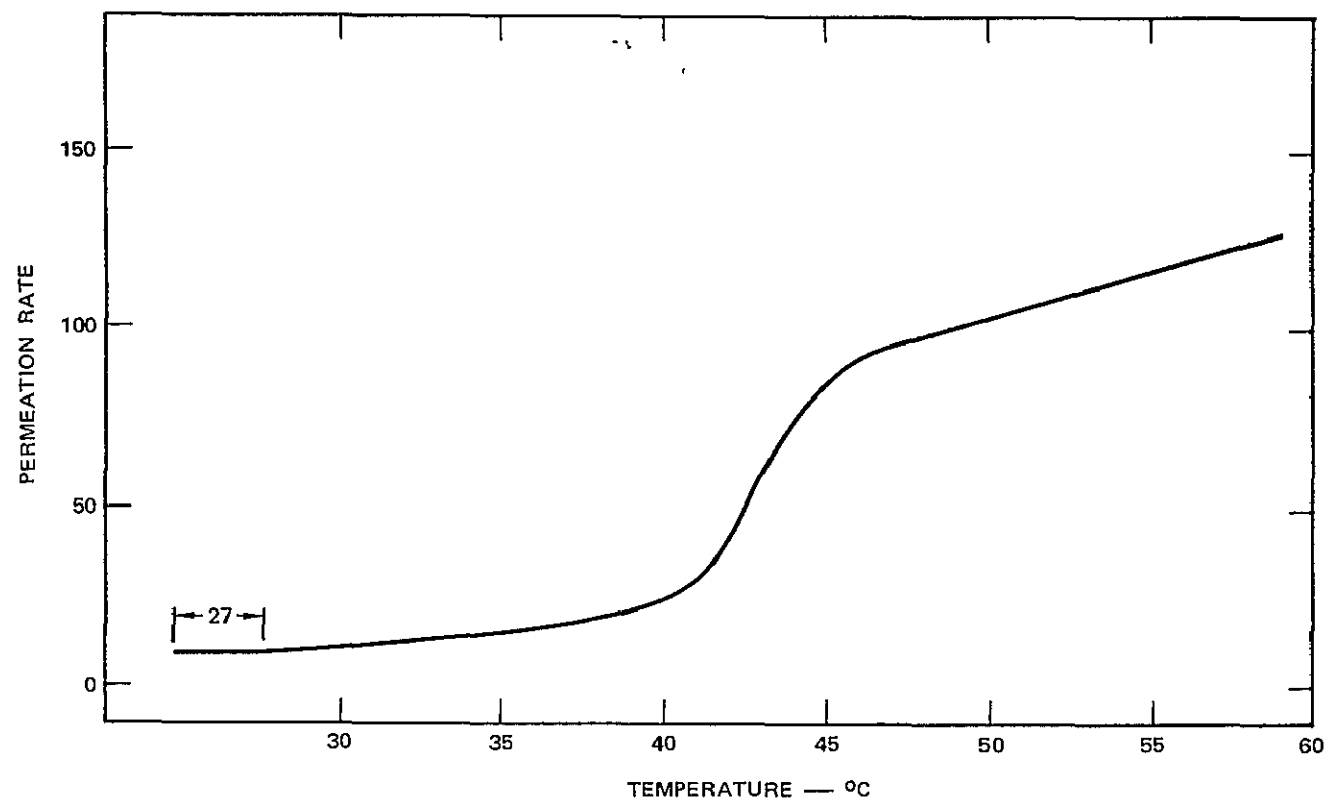


FIG 6



TA-321581-3

Figure 7